



This is a repository copy of *Theory of morphodynamic information processing: linking sensing to behaviour*.

White Rose Research Online URL for this paper:

<https://eprints.whiterose.ac.uk/202524/>

Version: Submitted Version

---

**Preprint:**

Juusola, M. [orcid.org/0000-0002-4428-5330](https://orcid.org/0000-0002-4428-5330), Takalo, J., Kemppainen, J. et al. (4 more authors) (Submitted: 2023) Theory of morphodynamic information processing: linking sensing to behaviour. [Preprint - Preprints.org] (Submitted)

<https://doi.org/10.20944/preprints202308.1210.v1>

---

© 2023 The Author(s). This is an open access article distributed under the Creative Commons Attribution License (<https://creativecommons.org/licenses/by/4.0/>) which permits unrestricted use, distribution, and reproduction in any medium, provided the original work is properly cited.

**Reuse**

This article is distributed under the terms of the Creative Commons Attribution (CC BY) licence. This licence allows you to distribute, remix, tweak, and build upon the work, even commercially, as long as you credit the authors for the original work. More information and the full terms of the licence here:

<https://creativecommons.org/licenses/>

**Takedown**

If you consider content in White Rose Research Online to be in breach of UK law, please notify us by emailing [eprints@whiterose.ac.uk](mailto:eprints@whiterose.ac.uk) including the URL of the record and the reason for the withdrawal request.



[eprints@whiterose.ac.uk](mailto:eprints@whiterose.ac.uk)  
<https://eprints.whiterose.ac.uk/>

Review

Not peer-reviewed version

---

# Theory of Morphodynamic Information Processing: Linking Sensing to Behaviour

---

[Mikko Juusola](#)<sup>\*</sup>, Jouni Takalo, Joni Kemppainen, Keivan Razban Haghighi, Ben Scales, James McManus, Lars Chittka

Posted Date: 16 August 2023

doi: 10.20944/preprints202308.1210.v1

Keywords: Vision; Information Theory; Neural Computation; Drosophila; Cognition; Compound Eye



Preprints.org is a free multidiscipline platform providing preprint service that is dedicated to making early versions of research outputs permanently available and citable. Preprints posted at Preprints.org appear in Web of Science, Crossref, Google Scholar, Scilit, Europe PMC.

Copyright: This is an open access article distributed under the Creative Commons Attribution License which permits unrestricted use, distribution, and reproduction in any medium, provided the original work is properly cited.

Review

# Theory of Morphodynamic Information Processing: Linking Sensing to Behaviour

Mikko Juusola <sup>1,\*</sup>, Jouni Takalo <sup>1</sup>, Joni Kemppainen <sup>1</sup>, Keivan Razban Haghghi <sup>1</sup>, Ben Scales <sup>1</sup>, James McManus <sup>1</sup> and Lars Chittka <sup>2</sup>

<sup>1</sup> School of Biosciences, University of Sheffield, Sheffield S10 2TN, UK

<sup>2</sup> Department of Biological and Experimental Psychology, School of Biological and Chemical Sciences, Queen Mary University of London, London E1 4NS, UK

\* Correspondence: Mikko Juusola, m.juusola@sheffield.ac.uk

**Summary:** The traditional understanding of brain function has predominantly focused on chemical and electrical processes. However, new research in fruit fly (*Drosophila*) binocular vision reveals ultrafast photomechanical photoreceptor movements significantly enhance information processing, thereby impacting a fly's perception of its environment and behaviour. The coding advantages resulting from these mechanical processes suggest that similar physical motion-based coding strategies may affect neural communication ubiquitously. The theory of neural morphodynamics proposes that rapid biomechanical movements and microstructural changes at the level of neurons and synapses enhance the speed and efficiency of sensory information processing, intrinsic thoughts, and actions by regulating neural information in a phasic manner. We propose that morphodynamic information processing evolved to drive predictive coding, synchronising cognitive processes across neural networks to match the behavioural demands at hand effectively.

**Keywords:** vision; information theory; neural computation; drosophila; cognition; compound eye

---

## Introduction

Behaviour arises from intrinsic changes in brain activity and responses to external stimuli, guided by animals' heritable characteristics and cognition that shape and adjust nervous systems to maximise survival. In this dynamic world governed by the laws of thermodynamics, brains are never static. Instead, their inner workings actively utilise and store electrochemical, kinetic, and thermal energy, constantly moving and adapting in response to intrinsic activity and environmental shifts orchestrated by genetic information encoded in DNA. However, our attempts to comprehend the resulting neural information sampling, processing, and codes often rely on stationarity assumptions and reductionist behaviour or reductionist brain activity analyses. Unfortunately, these preconceptions can prevent us from appreciating the role of rapid biomechanical movements and microstructural changes of neurons and synapses, which we call neural morphodynamics, in sensing and behaviours.

While electron-microscopic brain atlases provide detailed wiring maps at the level of individual synapses<sup>1-4</sup>, they fail to capture the continuous motion of cells. Fully developed neurons actively move, with their constituent molecules, molecular structures, dendritic spines and cell bodies engaging in twitching motions that facilitate signal processing and plasticity<sup>5-18</sup> (Figure 1A–D). Additionally, high-speed *in vivo* X-ray holography<sup>14</sup>, electrophysiology<sup>19</sup> and calcium-imaging<sup>10</sup> of neural activity suggest that ultrafast bursty or microsaccadic motion influences the release of neurotransmitter quanta, adding an extra layer of complexity to neuronal processing.

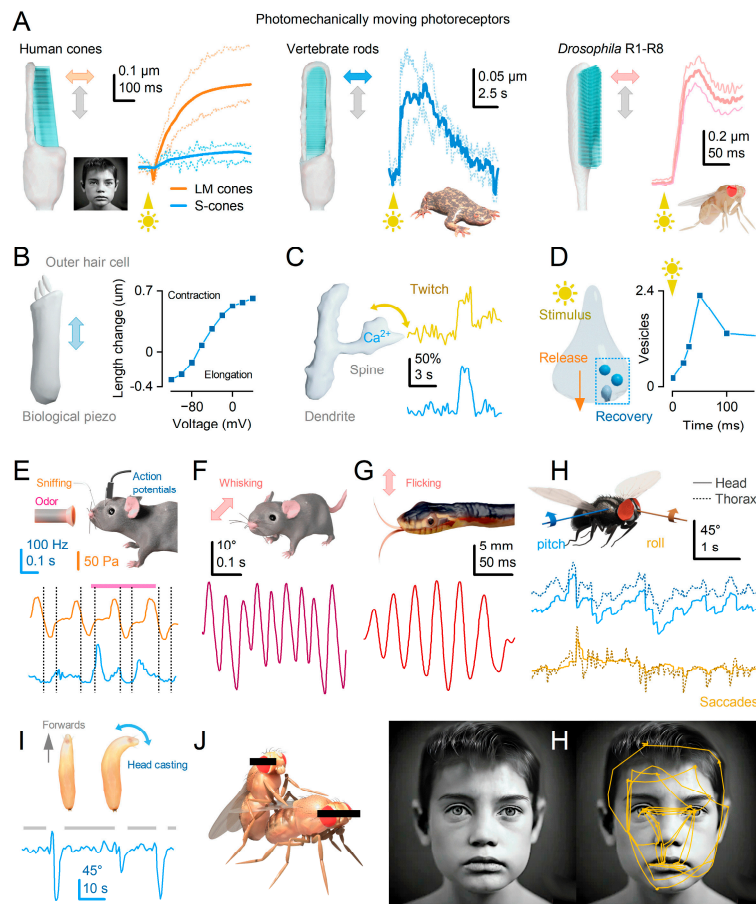


**Figure 1.** Sensory cells and central neurons, along with their morphodynamic components, dynamically respond to changes in information flow through phasic mechanical movements (A-D), exerting influence on sensory perception and behaviour (E-J). (A) Both vertebrate<sup>6,8</sup> and invertebrate photoreceptors<sup>7,8,12-14</sup> exhibit ultrafast photomechanical movements in response to changes in light intensity. (B) Outer hair cells<sup>20,21</sup> contract and elongate, amplifying variations in soundwave signals<sup>5</sup>. (C) Dendritic spines undergo twitching<sup>9,10</sup> motions while sampling synaptic information. (D) Synapses undergo ultrafast structural changes and tissue movements, actively participating in and optimising information transmission<sup>10,16-19,22-24</sup>. (E) Rats<sup>25,26</sup> and humans employ quick sniffs to enhance odour detection. (F) Fast whisking motion enhances the perception of environmental structure<sup>27</sup>. (G) Snakes flick their tongues to localise the source of odours better<sup>28</sup>. (H) Animals ranging from flies<sup>29</sup> to humans<sup>30</sup> utilise fast saccadic eye movements to observe the world<sup>31</sup>. (I) Larvae perform rapid head casting to determine the direction towards higher food concentration<sup>32,33</sup>. (J) Rhythmic sexual movements enhance tactile sensing and pleasure.

Recent findings on sensory organs and graded potential synapses provide compelling evidence for the crucial role of rapid morphodynamic changes in neural information sampling and synaptic communication<sup>6,8,12-14,19,23,34</sup>. In *Drosophila*, these phasic changes enhance performance and efficiency by synchronising responses to moving stimuli, effectively operating as a form of predictive coding<sup>12,14</sup>. These changes empower the small fly brain to achieve remarkable capabilities<sup>12-14</sup>, such as hyperacute stereovision<sup>14</sup> and time-normalised and aliasing-free responsiveness to naturalistic light contrasts of changing velocity, starting from photoreceptors and the first visual synapse<sup>12,35</sup>. Importantly, given the compound eyes' small size, these encoding tasks would only be physically possible with active movements<sup>12,14,35</sup>. Ultrafast photoreceptor microsaccades enable flies to perceive 2- and 3-dimensional patterns 4-10 times finer than the static pixelation limit imposed by photoreceptor spacing<sup>36,37</sup>. Thus, neural morphodynamics can be considered a natural extension of animals' efficient saccadic encoding strategy to maximise sensory information while linking perception with behaviour (Figure 1E-J)<sup>12,14,26-29,32</sup>.

Overarching questions remain: Are morphodynamic information sampling and processing prevalent across all brain networks, coevolving with morphodynamic sensing to amplify environmental perception, action planning, and behavioural execution? How does the genetic information, accumulated over hundreds of millions of years and stored in DNA, shape and drive brain morphodynamics to maximise the sampling and utilisation of sensory information within the biological neural networks of animals throughout their relatively short lifespans, ultimately improving fitness? Despite the diverse functions and morphologies observed in animals, operating similar molecular motors and reaction cascades within compartmentalised substructures by their neurons suggests that the morphodynamic code may be universal.

This review delves into this phenomenon, specifically focusing on recent discoveries in insect vision and visually guided behaviour. Insects have adapted to colonise all habitats except the deep sea, producing complex building behaviour and societies, exemplified by ants, bees, and termites. Furthermore, insects possess remarkable cognitive abilities that often rely on hyperacute perception. For instance, paper wasps can recognise individual faces among their peers<sup>38,39</sup>, while *Drosophila* can distinguish minute parasitic wasp females from harmless males<sup>40</sup>. These findings alone challenge the prevailing theoretical concepts<sup>41,42</sup>, as the visual patterns tested may occupy only a pixel or two if viewed from the experimental positions through static compound eyes. Instead, we elucidate how such heightened performance naturally emerges from ultrafast morphodynamics in sensory processing and behaviours<sup>12,14</sup>, emphasising their crucial role in enhancing perception and generating reliable neural representations of the variable world. Additionally, we propose underlying representational rules and general mechanisms governing morphodynamic sampling and information processing, to augment intelligence and cognition. We hope these ideas will pave the way for new insights and avenues in neuroscience research and our understanding of behaviour.

### Photoreceptor movements enhance vision

The structure and function of sense organs have long been recognised as factors that limit the quantity and variety of information they can gather<sup>36,41,43</sup>. However, a more recent insight reveals that the process of sensing itself is an active mechanism, utilising bursty or saccadic movements to enhance information sampling<sup>12-14,26,29,33,44-50</sup> (Figure 1). These movements encompass molecular, sensory cell, whole organ, head, and body motions, collectively and independently enhancing perception and behaviour.

Because compound eyes extend from the rigid head exoskeleton, appearing stationary to an outside observer, the *prima facie* is that their inner workings would also be immobile<sup>41,42,51</sup>. Therefore, as the eyes' ommatidial faceting sets their photoreceptor spacing, the influential static theory of compound eye optics postulates that insects can only see a "pixelated" low-resolution image of the world. According to this traditional static viewpoint, the ommatidial grid limits the granularity of the retinal image and visual acuity. Resolving two stationary objects requires at least three photoreceptors, and this task becomes more challenging when objects are in motion, further reducing visual acuity. The presumed characteristics associated with small static compound eyes, including large receptive fields, slow integration times, and spatial separation of photoreceptors, commonly attributed to spherical geometry, contribute to motion blur that impairs the detailed resolution of moving objects within the visual field<sup>41</sup>. As a result, male *Drosophila* relying on coarse visual information face a real dilemma in distinguishing between a receptive female fly and a hungry spider. To accurately differentiate, the male must closely approach the subject to detect distinguishing characteristics such as body shape, colour patterns, or movements. In this context, the difference between sex and death may hinge on an invisible line.

Recent studies on *Drosophila* have challenged the notion that fixed factors such as photoreceptor spacing, integration time, and receptive field size solely determine visual acuity<sup>12,14</sup>. Instead, these characteristics are dynamically regulated by photoreceptor photomechanics, leading to significant improvements in vision through morphodynamic processes. Intricate experiments (Figure 2A) have revealed that photoreceptors rapidly move in response to light intensity changes<sup>12-14</sup>. Referred to as high-speed photomechanical microsaccades<sup>12,14</sup>, these movements, which resemble a complex piston

motion (Figure 2B), occur in less than 100 milliseconds and involve simultaneous axial recoil and lateral swinging of the photoreceptors within a single ommatidium. These local morphodynamics result in adaptive optics (Figure 2C), enhancing spatial sampling resolution and sharpening moving light patterns over time by narrowing and shifting the photoreceptors' receptive fields<sup>12,14</sup>.

To understand the core concept and its impact on compound eye vision, let us compare the photoreceptors' receptive fields to image pixels in a digital camera (Figure 2E). Imagine shifting the camera sensor, capturing two consecutive images with a 1/2-pixel displacement. This movement effectively doubles the spatial image information. By integrating these two images over time, the resolution is significantly improved. However, if a pixel moves even further, it eventually merges with its neighbouring pixel (provided the neighbouring pixel remains still and does not detect changes in light). As a result of this complete pixel fusion, the acuity decreases since the resulting neural image will contain fewer pixels. Therefore, by restricting photoreceptors' micro-scanning to the interommatidial angle, *Drosophila* can effectively time-integrate a neural image that exceeds the optical limits of its compound eyes.

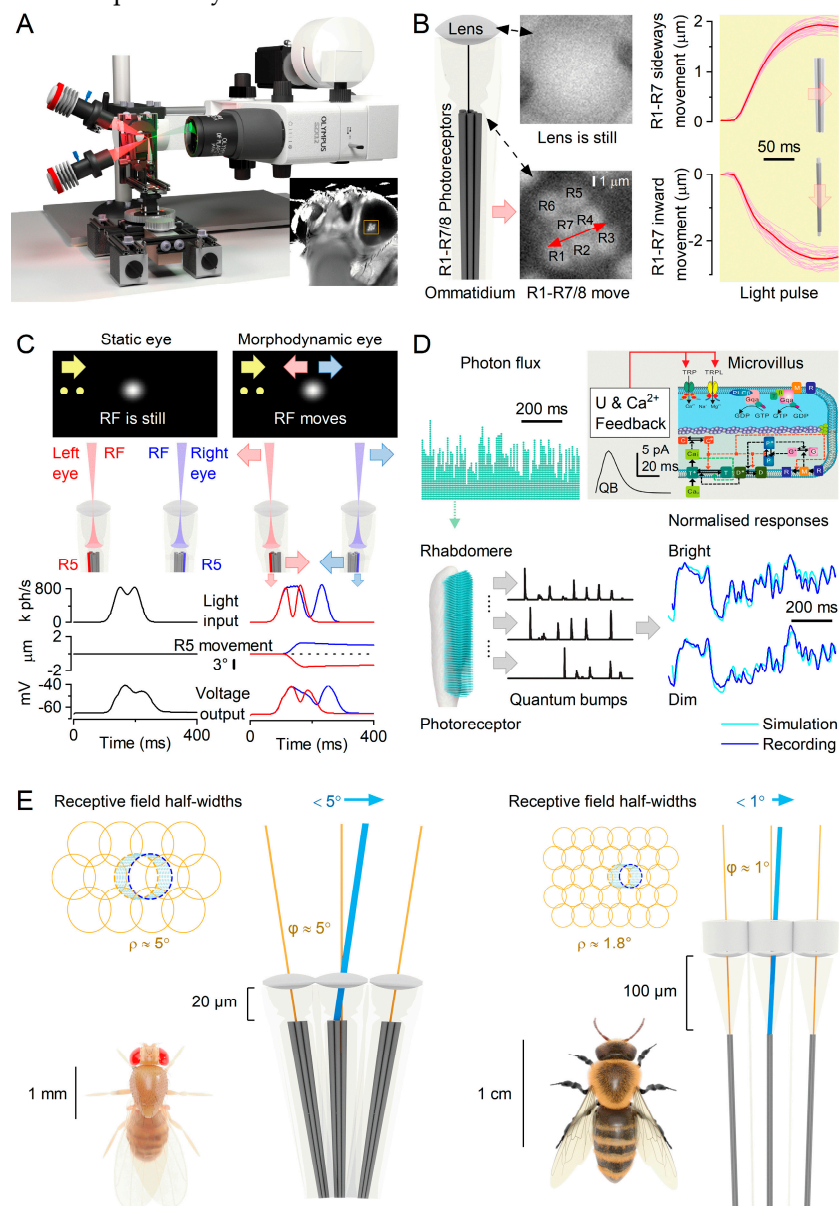


**Figure 2.** Photomechanical photoreceptor microsaccades enhance insect vision through adaptive compound eye optics. (A) High-speed infrared deep-pseudopupil microscopy<sup>13,14</sup> uncovers the intricate movement dynamics and specific directions of light-induced photoreceptor microsaccades across the compound eyes in living *Drosophila*. (B) During a microsaccade within an ommatidium, the

R1-R7/8 photoreceptors undergo rapid axial (inward) contraction and sideways movement along the R1-R2-R3 direction, executing a complex piston motion<sup>13,14</sup>. Meanwhile, the lens positioned above them, as an integral component of the rigid exoskeleton, remains stationary<sup>12</sup>. (C) When a moving light stimulus, such as two bright dots, traverses a photoreceptor's (shown for R5) receptive field (RF), the photoreceptor rapidly contracts away from the lens, causing the RF to narrow<sup>12,14</sup>. Simultaneously, the photoreceptor's swift sideways movement, aided by the lens acting as an optical lever, results in the RF moving in the opposite direction (of about 40-60°/s, illustrated here for movement with or against the stimuli). As a result, in a morphodynamic compound eye, the photoreceptor responses (depicted by blue and red traces) can detect finer and faster changes in moving stimuli than what the previous static compound eye theory predicts (represented by black traces). (D) Microsaccades result from photomechanical processes involving refractory photon sampling dynamics within the 30,000 microvilli<sup>7,12,14,52</sup>, which comprise the light-sensitive part of a photoreceptor known as the rhabdomere. Each microvillus encompasses the complete phototransduction cascade, enabling the conversion of successful photon captures into elementary responses called quantum bumps. This photomechanical refractory sampling mechanism empowers photoreceptors to consistently estimate changes in environmental light contrast across a wide logarithmic intensity range. The intracellularly recorded morphodynamic quantal information sampling and processing (represented by dark blue traces) can be accurately simulated under various light conditions using biophysically realistic stochastic photoreceptor sampling models (illustrated by cyan traces)<sup>12,14,53</sup>. (E) *Drosophila* photoreceptor microsaccades shift their rhabdomeres sideways by around 1-1.5  $\mu\text{m}$  (maximum < 2  $\mu\text{m}$ ), resulting in receptive field movements of approximately 3-4.5° in the visual space. The receptive field half-widths of R1-R6 photoreceptors cover the entire visual space, ranging from 4.5-6°. By limiting the micro-scanning to the interommatidial angle, *Drosophila* integrates a neural image that surpasses the optical limits of its compound eyes. Honeybee photoreceptor microsaccades shift their receptive fields by < 1°, smaller than the average receptive field half-width (~1.8°) at the front of the eye. This active sampling strategy in honeybees is similar to *Drosophila* and suggests that honeybee vision also surpasses the static pixelation limit of its compound eyes<sup>13</sup>.

### Microsaccades are photomechanical adaptations in phototransduction

*Drosophila* photoreceptors exhibit a distinctive toothbrush-like morphology characterised by their "bristled" light-sensitive structures known as rhabdomeres. In the outer photoreceptors (R1-6), there are approximately 30,000 bristles, called microvilli, which act as photon sampling units (Figure 2D)<sup>7,12,14</sup>. These microvilli collectively function as a waveguide, capturing light information across the photoreceptor's receptive field<sup>13,14</sup>. Each microvillus compartmentalises the complete set of phototransduction cascade reactions<sup>52</sup>, contributing to the refractive index and waveguide properties of the rhabdomere<sup>54</sup>. The phototransduction reactions within rhabdomeric microvilli of insect photoreceptors generate ultra-fast contractions of the whole rhabdomere caused by the PLC-mediated cleavage of PIP<sub>2</sub> headgroups (InsP<sub>3</sub>) from the microvillar membrane<sup>7,52</sup>. These photomechanics rapidly adjust the photoreceptor, enabling it to dynamically adapt its light input as the receptive field reshapes and interacts with the surrounding environment. Because photoreceptor microsaccades directly result from phototransduction reactions<sup>7,12,14,52</sup>, they are an inevitable consequence of compound eye vision. Without microsaccades, insects with microvillar photoreceptors would be blind<sup>7,12,14,52</sup>.

Insects possess an impressively rapid vision, operating approximately 3 to 15 times faster than our own. This remarkable ability stems from the microvilli's swift conversion of captured photons into brief unitary responses (Figure 2D; also known as quantum bumps<sup>52</sup>) and their ability to generate photomechanical micromovements<sup>7,12</sup> (Figure 2C). Moreover, the size and speed of microsaccades adapt to the microvilli population's refractory photon sampling dynamics<sup>12,53</sup> (Figure 2D). As light intensity increases, both the quantum efficiency and duration of photoreceptors' quantum bumps decrease<sup>53,55</sup>, resulting in more transient microsaccades<sup>12,14</sup>. These adaptations extend the dynamic range of vision<sup>53,56</sup> and enhance the detection of environmental contrast changes<sup>12,57</sup>, making visual objects highly noticeable under various lighting conditions. Consequently, *Drosophila* can perceive

moving objects across a wide range of velocities and light intensities, surpassing the resolution limits of the static eye's pixelation by 4-10 times (Figure 2E; the average inter-ommatidial angle,  $\varphi \approx 5^\circ$ )<sup>12,14</sup>.

Morphodynamic adaptations involving photoreceptor microvilli play a crucial role in insect vision by enabling rapid and efficient visual information processing. These adaptations lead to contrast-normalised (Figure 2D) and more phasic photoreceptor responses, achieved through significantly reduced integration time<sup>12,57,58</sup>. Evolution further refines these dynamics to match species-specific visual needs (Figure 2E). For example, honeybee microsaccades are smaller than those of *Drosophila*<sup>13</sup>, corresponding to the positioning of honeybee photoreceptors farther away from the ommatidium lenses. Consequently, reducing the receptive field size and interommatidial angles in honeybees is likely an adaptation that allows optimal image resolution during scanning<sup>13</sup>. Similarly, fast-flying flies such as houseflies and blowflies, characterised by a higher density of ommatidia in their eyes, are expected to exhibit smaller and faster photoreceptor microsaccades compared to slower-flying *Drosophila* with fewer and less densely packed ommatidia<sup>14</sup>. This adaptation enables the fast-flying flies to capture visual information with higher velocity<sup>53,57,59,60</sup> and resolution, albeit at a higher metabolic cost<sup>57</sup>.

### Matching saccadic behaviours to microsaccadic sampling

Photoreceptors' microsaccadic sampling likely evolved to align with animals' saccadic behaviours, maximising visual information capture<sup>12,14</sup>. Saccades are utilised by insects and humans to explore their environment (Figure 1J), followed by fixation periods where the gaze remains relatively still<sup>31</sup>. Previously, it was believed that detailed information was only sampled during fixation, as photoreceptors were thought to have slow integration times, causing image blurring during saccades<sup>31</sup>. However, fixation intervals can lead to perceptual fading through powerful adaptation, reducing visual information and potentially limiting perception to average light levels<sup>12,61,62</sup>. Therefore, to maximise information capture, fixation durations and saccade speeds should dynamically adapt to the statistical properties of the natural environment<sup>12</sup>. This sampling strategy would enable animals to efficiently adjust their behavioural speed and movement patterns in diverse environments, optimising vision—for example, moving slowly in darkness and faster in daylight<sup>12</sup>.

To investigate this theory, researchers studied the body yaw velocities of walking fruit flies<sup>63</sup> to sample light intensity information from natural images<sup>12</sup> (Figure 3). They found that saccadic viewing of these images improved the photoreceptors' information capture compared to linear or shuffled velocity walks<sup>12</sup>. This improvement was attributed to saccadic viewing generating bursty high-contrast stimulation, maximising the photoreceptors' ability to gather information. Specifically, the photomechanical and refractory phototransduction reactions of *Drosophila* R1-6 photoreceptors, associated with motion vision<sup>64</sup>, were found to be finely tuned to saccadic behaviour for sampling quantal light information, enabling them to capture 2-to-4-times more information in a given time compared to previous estimates<sup>12,55</sup>.

Further analysis, utilising multiscale biophysical modelling<sup>58</sup>, investigated the stochastic refractory photon sampling by 30,000 microvilli<sup>12</sup>. The findings revealed that the improved information capture during saccadic viewing can be attributed to the interspersed fixation intervals<sup>12,56</sup>. When fixating on darker objects, which alleviates microvilli refractoriness, photoreceptors can sample more information from transient light changes, capturing larger photon rate variations<sup>12</sup>. The combined effect of photomechanical photoreceptor movements and refractory sampling worked synergistically to enhance spatial acuity, reduce motion blur during saccades, facilitate adaptation during gaze fixation, and emphasise instances when visual objects crossed a photoreceptor's receptive field. Consequently, the encoding of high-resolution spatial information was achieved through the temporal mechanisms induced by physical motion<sup>12</sup>.

These discoveries underscore the crucial link between an animal's adaptation in utilising movements across different scales, ranging from nanoscale molecular dynamics to microscopic brain morphodynamics, to maximise visual information capture and acuity<sup>12</sup>. The new understanding from the *Drosophila* studies is that contrary to popular assumptions, neither saccades<sup>41</sup> nor fixations<sup>61</sup>



hinder the vision. Instead, they work together to enhance visual perception, highlighting the complementary nature of these active sampling movement patterns<sup>12</sup>.

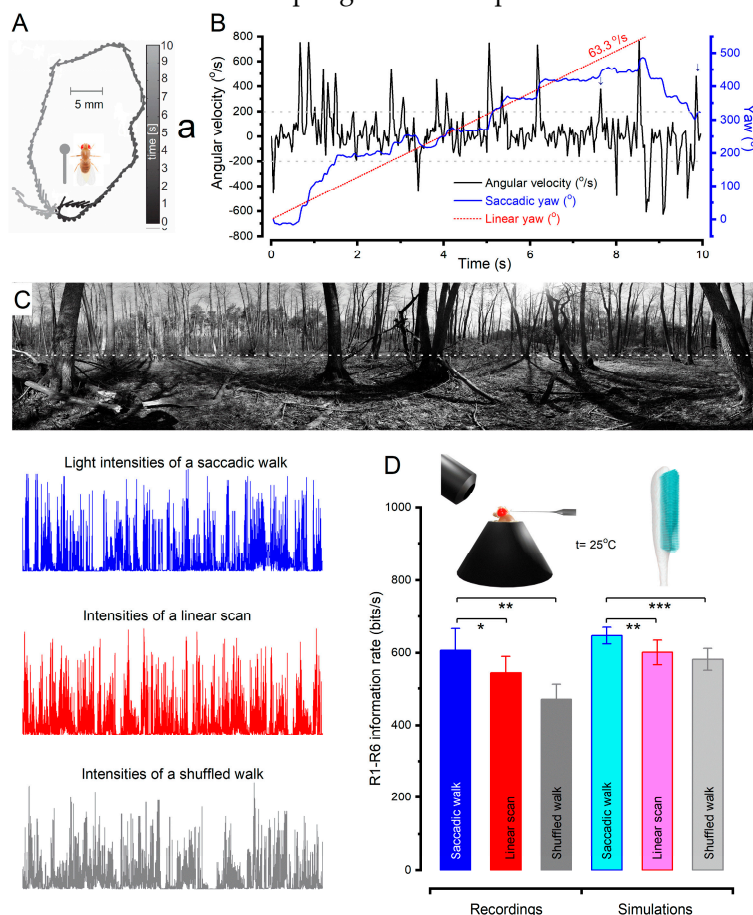


**Figure 3.** Saccadic Turns and Fixation Periods Enhance Information Extraction in *Drosophila*. (A) A representative walking trajectory of a fruit fly<sup>63</sup>. (B) Angular velocity and yaw of the recorded walk. (C) A 360° natural scene utilised to generate three distinct time series of light intensity<sup>12</sup>. The dotted white line indicates the intensity plane employed during the walk. The blue trace represents a light intensity time series generated by overlaying the walking fly's yaw dynamics (A-B) onto the scene. The red trace corresponds to a light intensity time series obtained by scanning the scene at the median velocity of the walk (linear: 63.3°/s). The grey trace depicts a light intensity time series obtained using shuffled walking velocities. Brief saccades and longer fixation periods introduce burst-like patterns to the light input. (D) These light intensity time series were employed as stimuli in intracellular photoreceptor recordings and simulations using a biophysically realistic stochastic photoreceptor model. Both the recordings and simulations showed that saccadic viewing enhances information transmission in R1-R6 photoreceptors, indicating that this mechanism has evolved with refractory photon sampling to maximise information capture from natural scenes<sup>12</sup>.

### Left and right eyes' mirror-symmetric microsaccades are tuned to optic flow

When *Drosophila* encounters moving objects in natural environments, its left and right eye photoreceptor pairs generate microsaccadic movements that synchronise their receptive field scanning in opposite directions (Figure 4)<sup>12,14</sup>. To quantitatively analyse these morphodynamics, researchers utilised a custom-designed high-speed microscope system<sup>13</sup>, tailored explicitly for recording photoreceptor movements within insect compound eyes (Figure 2A). Using infrared illumination, which flies cannot see, the positions and orientations of photoreceptors in both eyes were measured, revealing mirror-symmetric angular orientations between the eyes and symmetry within each eye (Figure 4A). It was discovered that a single point in space within the frontal region, where receptive fields overlap (Figure 4B), is detected by at least 16 photoreceptors, eight in each. This highly ordered mirror-symmetric rhabdomere organisation, leading to massively over-complete

tiling of the eyes' binocular visual fields<sup>14</sup> (Figure 4C), challenges the historical belief that small insect eyes, such as those of *Drosophila*, are optically too coarse and closely positioned to support stereovision<sup>41</sup>.

By selectively stimulating the rhabdomeres with targeted light flashes, researchers determined the specific photomechanical contraction directions for each eye's location (Figure 4D). Analysis of the resulting microsaccades enabled the construction of a 3D-vector map encompassing the frontal and peripheral areas of the eyes. These microsaccades exhibited mirror symmetry between the eyes and aligned with the rotation axis of the R1-R2-R3 photoreceptor of each ommatidium (Figure 4D, left), indicating that the photoreceptors' movement directions were predetermined during development (Figure 4A)<sup>13,14</sup>. Strikingly, the 3D-vector map representing the movements of the corresponding photoreceptor receptive fields (Figure 4D) coincides with the optic flow-field generated by the fly's forward thrust (Figure 4E)<sup>13,14</sup>. This alignment provides microsaccade-enhanced detection and resolution of moving objects (cf. Figure 2C) across the extensive visual fields of the eyes (approximately 360°), suggesting an evolutionary optimisation of fly vision for this intriguing capability.

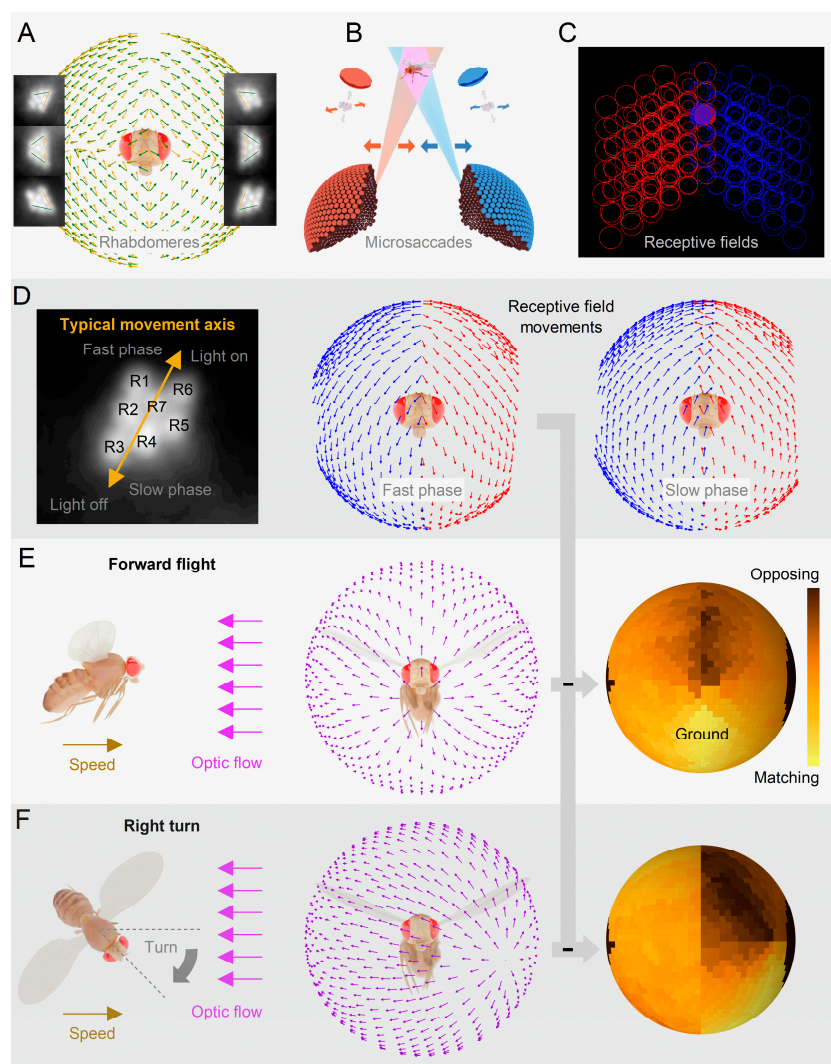


**Figure 4.** The mirror-symmetric ommatidial photoreceptor arrangement and morphodynamics of the left and right eyes enhance detection of moving objects during visual behaviours. (A) The photoreceptor rhabdomere patterns of the ommatidial left and right eyes (inset images) exhibit horizontal and ventral mirror symmetry, forming a concentrically expanding diamond shape<sup>13,14,65</sup>. (B) When a moving object, such as a fly, enters the receptive fields (RFs) of the corresponding frontal left and right photoreceptors (indicated by red and blue beams), the resulting light intensity changes cause the photoreceptors to contract mirror-symmetrically. (C) The half-widths of the frontal left and

right eye R6 photoreceptors' RFs (disks), projected 5 mm away from the eyes. Red circles represent the RFs of neighbouring photoreceptors in the left visual field, blue in the right. (D) Contraction (light-on) moves R1-R7/8 photoreceptors (left) in R3-R2-R1 direction (fast phase), recoil (light-off) returns them in opposite R1-R2-R3 direction (slow phase)<sup>13,14</sup>. The corresponding fast-phase (centre) and slow-phase (right) RF vector maps. (E) The fast-phase RF map compared to the forward flying fly's optic flow field (centre), as experienced with the fly head upright<sup>14</sup>. Their difference (error) is shown right. The fast phase matches the ground flow, while the opposite slow phase matches the sky flow<sup>14</sup>. (F) During yaw rotation, the mirror-symmetric movement of the photoreceptor RFs in the left and right eyes enhances the binocular contrast differences in the surrounding environment.

The microsaccadic receptive field movements comprise a fast phase (Figure 4D, left) aligned with the flow-field direction during light-on (Figure 4D, middle), followed by a slower phase in the opposite direction during light-off (Figure 4D, right). When a fly is in forward flight with an upright head (Figure 4E, left and middle), the fast and slow phases reach equilibrium (Figure 4E, right). The fast phase represents "ground-flow," while the slower phase represents "sky-flow." In the presence of real-world structures, locomotion enhances sampling through a push-pull mechanism. Photoreceptors transition between fast and slow phases, thereby collectively improving neural resolution over time<sup>14</sup> (Figure 2C). Fast microsaccades are expected to aid in resolving intricate visual clutter, whereas slower microsaccades enhance the perception of the surrounding landscape and sky<sup>14</sup>. Moreover, this eye-location-dependent orientation-tuned bidirectional visual object enhancement makes any moving object deviating from the prevailing self-motion-induced optic flow field stand out. Insect brains likely utilise the resulting phasic neural image contrast differences to detect or track predator movements or conspecifics across the eyes' visual fields. For example, this mechanism could help a honeybee drone spot and track the queen amidst a competing drone swarm<sup>66</sup>, enabling efficient approach and social interaction.

Rotation (yaw) (Figure 4F, left and middle) further enhances binocular contrasts (Figure 4F, right), with one eye's phases synchronised with field rotation while the other eye's phases exhibit the reverse pattern<sup>14</sup>. Many insects, including bees and wasps, engage in elaborately patterned learning or homing flights, involving fast saccadic turns and bursty repetitive waving, when leaving their nest or food sources<sup>67,68</sup> (Figure 4G). Given the mirror-symmetry and ultrafast photoreceptor microsaccades of bee eyes<sup>13</sup>, these flight patterns are expected to drive enhanced binocular detection of behaviourally relevant objects, landmarks, and patterns, utilising the phasic differences in microsaccadic visual information sampling between the two eyes<sup>12,14</sup>. Thus, learning flight behaviours likely make effective use of optic-flow-tuned and morphodynamically enhanced binocular vision, enabling insects to navigate and return to their desired locations successfully.

### Mirror-symmetric microsaccades enable 3d vision

Crucially, *Drosophila* uses mirror-symmetric microsaccades to sample the three-dimensional visual world, enabling the extraction of depth information (Figure 5). This process entails comparing the resulting morphodynamically sampled neural images from its left and right eye photoreceptors<sup>14</sup>. The disparities in  $x$ - and  $y$ -coordinates between corresponding "pixels" provide insights into scene depth. In response to light intensity changes, the left and right eye photoreceptors contract mirror-symmetrically, narrowing and sliding their receptive fields in opposing directions, thus shaping neural responses (Figure 5A; also see Figure 2C)<sup>12,14</sup>. By cross-correlating these photomechanical responses between neighbouring ommatidia, the *Drosophila* brain is predicted to achieve a reliable stereovision range spanning from less than 1 mm to approximately 150 mm<sup>14</sup>. The crucial aspect lies in utilising the responses' phase differences as temporal cues for perceiving 3D space (Figure 5A,B). Furthermore, researchers assessed if a static *Drosophila* eye model with immobile photoreceptors could discern depth<sup>14</sup>. These calculations indicate that the lack of scanning activity by the immobile photoreceptors and the small distance between the eye (Figure 5A,  $k = 440 \mu\text{m}$ ) would only enable a significantly reduced depth perception range, underlining the physical and evolutionary advantages of moving photoreceptors in depth perception.

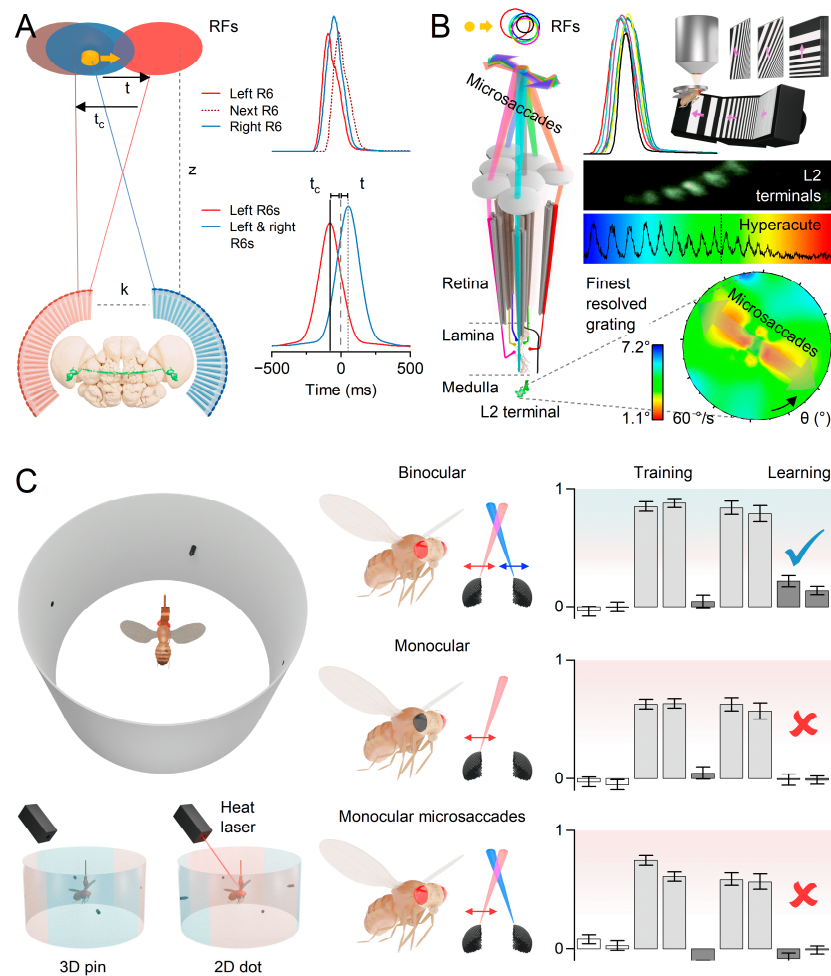


**Figure 5.** *Drosophila* visual behaviours exhibit hyperacute 3D vision, aligning with morphodynamic compound eye modelling. (A) *Drosophila* compound eyes' depth perception constraints and the computations for morphodynamic triangulation of object depth ( $z$ )<sup>14</sup>.  $k$  is the distance between the corresponding left and right eye photoreceptors, and  $t$  is their time-delay.  $t_c$  is the time-delay between the neighbouring photoreceptors in the same eye. The left eye is represented by the red receptive field (RFs), while the right eye is represented by the blue RF. Simulated voltage responses (top) of three morphodynamically responding R6-photoreceptors when a  $1.7^\circ \times 1.7^\circ$  object (orange) moves across their overlapping RFs at a speed of  $50^\circ/\text{s}$  and a distance of 25 mm. The corresponding binocular cross-correlations (bottom) likely occur in the retinotopically organised neural cartridges of the lobula optic lobe, where location-specific ipsi- and contralateral photoreceptor information is pooled (green LC14 neuron<sup>14</sup>). Time delays between the maximum correlations (vertical lines) and the moment the object crosses the RF centre of the left R6-photoreceptor (vertical dashed line). (B) In neural superposition wiring<sup>69</sup>, the R1-6 photoreceptors originating from six neighbouring ommatidia sample a moving stimulus (orange dot). Their overlapping receptive fields (RFs; coloured rings) swiftly bounce along their predetermined microsaccade directions (coloured arrows; see also Figure 4D) as the photoreceptors transmit information to large monopolar cells (LMC, specifically L1-L3, with L2 shown) and the lamina amacrine cells. While R7/8 photoreceptors share some information with R1 and R6 through gap junctions<sup>70</sup> R7/8 establish synapses in the medulla. Simulations reveal the superpositional R1-R7/8s' voltage responses (coloured traces) with their phase differences when a  $1.7^\circ \times 1.7^\circ$  dot traverses their receptive fields at  $100^\circ/\text{s}$  (orange dot). 2-photon imaging of L2 terminals'  $\text{Ca}^{2+}$ -responses to a dynamically narrowing black-and-white grid that moves in different directions shows L2 monopolar cells generating hyperacute ( $<5^\circ$ ; cf. Figure 2B,C,E) responses along the same microsaccade movement axis (coloured arrows) of the superpositioned photoreceptors that feed information to them (cf. Figure 4). (C) In a visual learning experiment, a tethered, head-immobilised *Drosophila* flies in a flight simulator. The fly was positioned at the centre of a panoramic arena to

prevent it from perceiving motion parallax cues<sup>14</sup>. The arena features two hyperacute dots placed 180° apart and two equally sized 3D pins positioned perpendicular to the dots. The fly generates subtle yaw torque signals to indicate its intention to turn left or right, allowing it to explore the visual objects within the arena. These signals are used to rotate the arena in the opposite direction of the fly's intended turns, establishing a synchronised feedback loop. During the training phase, a heat punishment signal is associated with either the dot or 3D pin stimulus, smaller than an ommatidial pixel at this distance, delivered through an infrared laser. After training, without any heat punishment, the extent to which the fly has learned to avoid the tested stimulus is measured. Flies with normal binocular vision (above) exhibit significant learning scores, indicating their ability to see the dots and the pins as different objects. However, flies with monocular vision (one eye painted black, middle) or mutants that exhibit lateral photoreceptor microsaccades only in one eye (below) cannot learn this task. These results show that *Drosophila* has hyperacute stereovision<sup>14</sup>.

Behavioural experiments in a flight simulator verified that *Drosophila* possesses hyperacute stereovision<sup>14</sup> (Figure 5C). Tethered head-fixed flies were presented with 1-4° 3D and 2D objects, smaller than their eyes' average interommatidial angle (cf. Figure 2E). Notably, the flies exhibited a preference for fixating on the minute 3D objects, providing support for the new morphodynamic sampling theory of hyperacute stereovision.

In subsequent learning experiments, the flies underwent training to avoid specific stimuli, successfully showing the ability to discriminate between small ( $\ll 4^\circ$ ) equal-contrast 3D and 2D objects. Interestingly, because of their immobilised heads, flies could not rely on motion parallax signals during learning, meaning the discrimination relied solely on the eyes' image disparity signals. Flies with one eye painted over and mutants, incapable of producing photoreceptor microsaccades' sideways movement in one eye, failed to learn the stimuli. These results firmly establish the significance of binocular mirror-symmetric photoreceptor microsaccades in sampling 3D information. Further investigations revealed that the R1-6 (associated with motion vision<sup>64</sup>) and R7/R8 (associated with colour vision<sup>71</sup>) photoreceptor classes contribute to hyperacute stereopsis. The findings provide compelling evidence that mirror-symmetric microsaccadic sampling, as a form of ultrafast neural morphodynamics, is necessary for hyperacute stereovision in *Drosophila*<sup>14</sup>.

### Reliable neural estimates of the variable world

The heterogeneous nature of the fly's retinal sampling matrix—characterised by varying rhabdomere sizes<sup>12</sup> (Figures 4, 5B and 6A), random distributions of visual pigments<sup>72</sup> (Figure 6A), variations in photoreceptor synapse numbers<sup>3</sup> (Figure 6A), the stochastic integration of single photon responses<sup>53,55,73</sup> (quantum bumps) (Figure 2D)<sup>12,56,58</sup> and stochastic variability in microsaccade waveforms<sup>12-14</sup> - eliminates spatiotemporal aliasing<sup>12,14</sup> (Figure 6B), enabling reliable transmission of visual information (Figures 2C,D, 3D and 5B). Thus, the morphodynamic information sampling theory<sup>12,14</sup> challenges previous assumptions of *static* compound eyes<sup>41</sup>. These assumptions suggested that the ommatidial grid of immobile photoreceptors structurally limits spatial resolution, rendering the eyes susceptible to undersampling the visual world and prone to aliasing<sup>41</sup>.

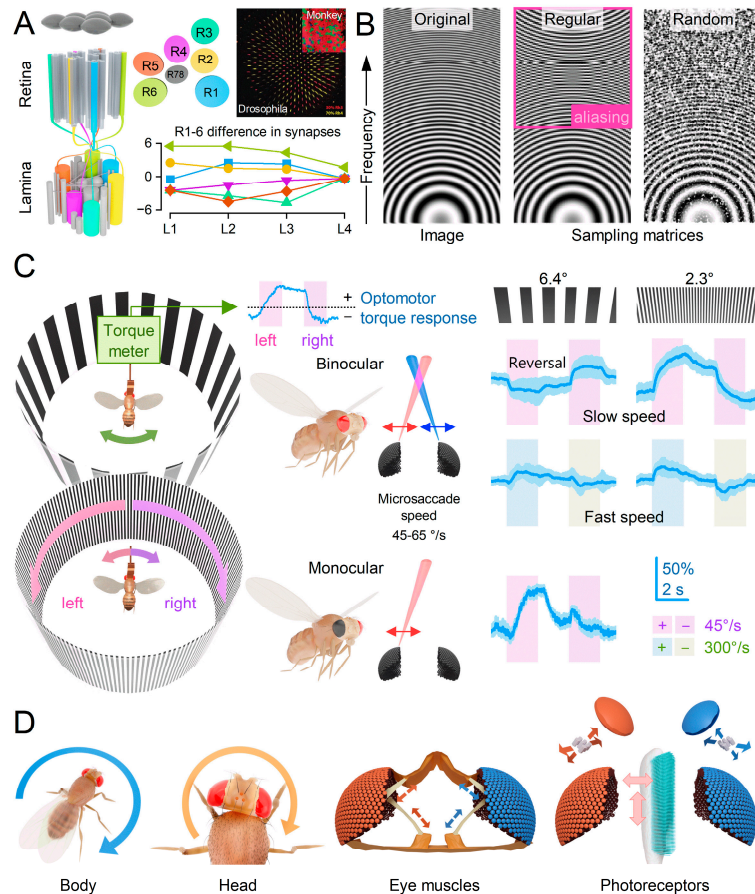


**Figure 6.** Stochasticity and variations in the ommatidial photoreceptor grid structure and function combat spatiotemporal aliasing in morphodynamic information sampling and processing. (A) *Drosophila* R1-R7/8 photoreceptors are differently sized and asymmetrically positioned<sup>12,14</sup>, forming different numbers of synapses with interneurons<sup>3</sup> (L1-L4). Moreover, R7y and R7p receptors' colour sensitivity<sup>74</sup> establishes a random-like sampling matrix, consistent with anti-aliasing sampling<sup>12,75</sup>. The inset shows similar randomisation for macaque retina<sup>76</sup> (red, green and blue cones) (B) Demonstration of how a random sampling matrix eliminates aliasing<sup>12</sup>. An original  $\sin(x^2 + y^2)$  image in 0.1 resolution. Under-sampling this image with 0.2 resolution by a regular matrix leads to aliasing: ghost rings appear, which the nervous system cannot differentiate from the original real image. Sampling the original image with a 0.2 resolution random matrix loses some of its fine resolution due to broadband noise, but sampling is aliasing-free. (C) In the flight simulator optomotor paradigm, a tethered head-fixed *Drosophila* robustly responds to hyperacute stimuli (tested from  $\sim 0.5^\circ$  to  $\sim 4^\circ$  wavelengths) for different velocities (tested from  $30^\circ/\text{s}$  to  $500^\circ/\text{s}$ ). However, flies show a response reversal to  $45^\circ/\text{s}$  rotating  $6.4^\circ$ -stripe panorama. In contrast, monocular flies, with one eye painted black, do not reverse their optomotor responses, indicating that the reversal response is not induced by spatial aliasing<sup>14</sup>. (D) The compound eyes' active stereo information sampling involves body and head movements, global retina movements, and local photomechanical photoreceptor microsaccades.

Supporting the new morphodynamic theory<sup>12,14</sup>, tethered head-fixed *Drosophila* exhibit robust optomotor behaviour in a flight simulator system (Figure 6C). The flies generated yaw torque responses, represented by the blue traces, indicating their intention to follow the left or right turns of the stripe panorama. These responses are believed to be a manifestation of an innate visuomotor reflex aimed at minimising retinal image slippage<sup>41,77</sup>. Consistent with *Drosophila*'s hyperacute ability to differentiate small 3D and 2D objects<sup>14</sup> (Figure 5C), the tested flies reliably responded to rotating panoramic black-and-white stripe scenes with hyperacute resolution, tested down to  $0.5^\circ$  resolution<sup>12,14</sup>. This resolution is about ten times finer than the eyes' average interommatidial angle

(Figure 2E), significantly surpassing the explanatory power of the traditional *static* compound eye theory<sup>41</sup>, which predicts 4°-5° maximum resolvability.

However, when exposed to slowly rotating 6.4-10° black-and-white stripe waveforms, a head-fixed tethered *Drosophila* displays reversals in its optomotor flight behaviour<sup>14</sup> (Figure 6C). Previously, this optomotor reversal was thought to result from the static ommatidial grid spatially aliasing the sampled panoramic stripe pattern due to the stimulus wavelength being approximately twice the eyes' average interommatidial angle (Figure 2E). Upon further analysis, the previous interpretation of these reversals as a sign of aliasing<sup>41,45</sup> is contested. Optomotor reversals primarily occur at 40-60°/s stimulus velocities, matching the speed of the left and right eyes' mirror-symmetric photoreceptor microsaccades<sup>14</sup> (Figures 6C and 2C). As a result, one eye's moving photoreceptors are more likely to be locked onto the rotating scene than those in the other eye, which move against the stimulus rotation. This discrepancy creates an imbalance that the fly's brain may interpret as the stimulus rotating in the opposite direction<sup>14</sup>.

Notably, the optomotor behaviour returns to normal when the tested fly has monocular vision (with one eye covered) and during faster rotations<sup>14</sup> or finer stripe pattern waveforms<sup>12,14</sup> (Figure 6C). Therefore, the abnormal optomotor reversal, which arises under somewhat abnormal and specific stimulus conditions when tested with head-fixed and position-constrained flies, must reflect high-order processing of binocular information and cannot be attributed to spatial sampling aliasing that is velocity and left-vs-right eye independent<sup>14</sup>.

### Multiple layers of active sampling vs simple motion detection models

In addition to photoreceptor microsaccades, insects possess intraocular muscles capable of orchestrating coordinated oscillations of the entire photoreceptor array, encompassing the entire retina<sup>12,14,45,78</sup> (Figure 6D). This global motion has been proposed as a means to achieve super-resolution<sup>79,80</sup>, but not for stereopsis. While the muscle movements alter the light patterns reaching the eyes, leading to the occurrence of photoreceptor microsaccades, it is the combination of local microsaccades and global retina movements, which include any body and head movements<sup>29,44,68,81</sup> (Figure 6D), that collectively govern the active sampling of stereoscopic information by the eyes<sup>12-14</sup>.

The *Drosophila* brain effectively integrates depth and motion computations using mirror-symmetrically moving image disparity signals from binocular vision channels<sup>14</sup>. Previous assumptions that insect brains perform high-order computations on low-resolution sample streams from their static eyes are now being questioned. For instance, the motion detection ideals of reduced input-output systems<sup>64,82</sup>, such as Hassenstein-Reichardt<sup>83</sup> and Barlow-Levick<sup>84</sup> models, require updates to incorporate ultrafast morphodynamics<sup>12-14</sup> and state-dependent synaptic processing<sup>85-89</sup>. The updates are crucial as these processes actively shape neural responses, perception, and behaviors<sup>86</sup>, providing essential ingredients of hyperacute 3D vision<sup>12,14,38,40</sup> and intrinsic decision-making<sup>12,14,90-92</sup> that occur in a closed-loop interaction with the changing environment.

Accumulating evidence, consistent with the idea that brains reduce uncertainty by synchronously integrating multisensory information<sup>93</sup>, further suggests that object colour and shape information partially streams through the same channels previously thought to be solely for motion information<sup>70</sup>. Consequently, individual neurons within these channels should engage in multiple parallel processing tasks<sup>70</sup>, adapting in a phasic and goal-oriented manner. These emerging concepts challenge oversimplified input-output models of insect vision, highlighting the importance of ultrafast neural morphodynamics and active vision in perception and behaviour.

### Benefits of neural morphodynamics

Organisms have adapted to the quantal nature of the dynamic physical world, resulting in ubiquitous active use of quantal morphodynamic processes and signalling within their constituent parts (cf. Figure 1). Besides enhancing information sampling and flow in sensory systems for efficient perception<sup>5-8,12-15</sup>, we propose that ultrafast neural morphodynamics likely evolved universally to facilitate effective communication across nervous systems<sup>9-11,23</sup>. By aligning with the moving world principles of thermodynamics and information theory<sup>94-96</sup>, the evolution of nervous systems

harnesses neural morphodynamics to optimise perception and behavioural capabilities, ensuring efficient adaptation to the ever-changing environment. The benefits of ultrafast morphodynamic neural processing are substantial and encompass the following (Figure 7):

### **Efficient Neural Encoding of Reliable Representations across Wide Dynamic Range**

Neural communication through synapses relies on rapid pre- and postsynaptic ultrastructural movements that facilitate efficient quantal release and capture of neurotransmitter molecules<sup>19,22,23</sup>. These processes share similarities with how photoreceptor microvilli have evolved to utilise photomechanical movements<sup>12-14</sup> with quantal refractory photon sampling<sup>12,53,56</sup> to maximise information in neural responses (Figure 3D). In both systems, ultrafast morphodynamics are employed with refractoriness to achieve highly accurate sampling of behaviourally or intrinsically relevant information by rapidly adapting their quantum efficiency to the influx of vastly varying sample (photon vs neurotransmitter molecule) rate changes<sup>12,14,53,56</sup>.

In synaptic transmission (Figure 1D), presynaptic transmitter vesicles are actively transported to docking sites by molecular motors<sup>18</sup>. Within these sites, vesicle depletion occurs through ultrafast exocytosis, followed by replenishment via endocytosis<sup>23</sup>. These processes generate ultrastructural movements, vesicle queuing and refractory pauses<sup>18</sup>. Such movements and pauses occur as vesicle numbers, and potentially their sizes<sup>19</sup>, adapt to sensory or neural information flow changes. Given that a spherical vesicle contains many neurotransmitter molecules with a high rate of release, the transmitter molecules, acting as carriers of information, can exhibit logarithmic changes from one moment to another. Conversely, the adaptive morphodynamic processes at the postsynaptic sites involve rapid movements of dendritic spines<sup>10</sup> (cf. Figure 1C) or transmitter-receptor complexes<sup>18</sup>. These ultrastructural movements likely facilitate efficient sampling of information from the rapid changes in neurotransmitter concentration, enabling swift and precise integration of macroscopic responses from the sampled postsynaptic quanta<sup>19,22</sup>.

Interestingly, specific circuits have evolved to integrate synchronous high signal-to-noise information from multiple adjacent pathways, thereby enhancing the speed and accuracy of phasic signals<sup>19,22,24,35,97</sup>. This mechanism is particularly beneficial for computationally challenging tasks, such as distinguishing object boundaries from the background during variable self-motion. For instance, in the photoreceptor-LMC synapse, the fly eye exhibits neural superposition wiring<sup>69</sup> (Figure 7A), allowing each LMC to simultaneously sample and integrate quantal events from six neighbouring photoreceptors (R1-6). Because the receptive fields of these photoreceptors only partially overlap and move in slightly different directions during microsaccades, each photoreceptor conveys a distinct phasic aspect of the visual stimulus to the LMCs<sup>14</sup> (L1-3; cf. Figure 5B). The LMCs actively differentiate these inputs, resulting in rapidly occurring phasic responses with notably high signal-to-noise ratios, particularly at high frequencies<sup>19,22,24,35</sup>.



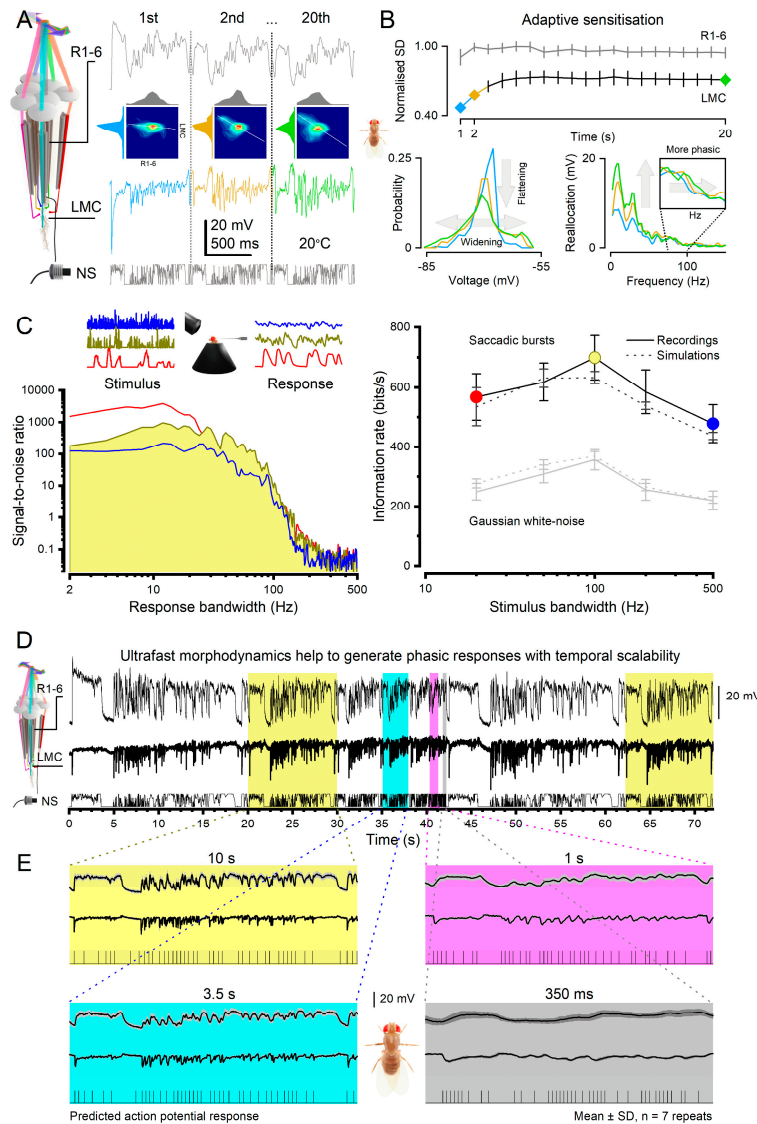


**Figure 7.** Pre- and postsynaptic morphodynamic sampling adapt to optimise information allocation in neural channels. (A) Adaptation enhances sensory information flow over time. R1–6 photoreceptor (above) and LMC voltage responses (below), as recorded intracellularly from *Drosophila* compound eyes in vivo, to a repeated naturalistic stimulus pattern, NS<sup>35</sup>. The recordings show how these neurons’ information allocation changes over time (for 1<sup>st</sup>, 2<sup>nd</sup> and 20<sup>th</sup> s of stimulation). The LMC voltage modulation grows rapidly over time, whereas the photoreceptor output changes less, indicating that most adaptation in the phototransduction occurs within the first second. Between these traces are their probability and the joint probability density functions (“hot” colours denote high probability). Notably, the mean synaptic gain increases dynamically; white lines highlight its steepening slope during repetitive NS<sup>35</sup>. (B) LMC output sensitises dynamically<sup>35</sup>: its probability density flattens and widens over time (arrows), causing a time-dependent upwards trend in standard deviation (SD). Simultaneously, its frequency distribution changes. Because both its low- (up arrow) and high-frequency (up right) content increases while R1-6 output is less affected, the synapse allocates information more evenly within the LMC bandwidth over time. (C) Left: Signal-to-noise ratio (SNR) of *Drosophila* R1-6 photoreceptor responses to 20 Hz (red), 100 Hz (yellow), and 500 Hz (blue) saccade-like contrast bursts<sup>12</sup>. SNR increases with contrast (right) and reaches its maximum value (~6,000) for 20 Hz bursts (red, left), while 100 Hz bursts (yellow) exhibit the broadest frequency range. Right: Information transfer rate comparisons between photoreceptor recordings and stochastic model simulations for saccadic light bursts and Gaussian white noise stimuli of varying bandwidths<sup>12</sup>. The estimated information rates from both recorded and simulated data closely correspond across the

entire range of encoding tested. This indicates that the morphodynamic refractory sampling (as performed by 30,000 microvilli) generates the most information-rich responses to saccadic burst stimulation. (D) Adaptation to repetitive naturalistic stimulation shows phasic scale-invariance to pattern speed. 10,000 points-long naturalistic stimulus sequence (NS) was presented and repeated at different playback velocities, lasting from 20 s (0.5 kHz) to 333 ms (30kHz)<sup>35</sup>. The corresponding intracellular photoreceptor (top trace) and LMC (middle trace) voltage responses are shown. The coloured sections highlight stimulus-specific playback velocities used during continuous recording. (E) The time-normalised shapes of the photoreceptor (above) and LMC (below) responses depict similar aspects of the stimulus, regardless of the playback velocity used (ranging from 0.5 to 30 kHz)<sup>35</sup>. The changes in the naturalistic stimulus speed, which follow the time-scale invariance of 1/f statistics, maintain the power within the frequency range of LMC responses relatively consistent. Consequently, LMCs can integrate similar size responses (contrast constancy) for the same stimulus pattern, irrespective of its speed<sup>35</sup>. These responses are predicted to drive generation of self-similar (scalable) action potential representations of the visual stimuli in central neurons.

Moreover, in this system, coding efficiency improves dynamically by adaptation, which swiftly flattens and widens the LMC's amplitude and frequency distributions over time<sup>19,22</sup> (Figure 7B), improving sensitivity to under-represented signals within seconds. Such performance implies that LMCs strive to utilise their output range equally in different situations since a message in which every symbol is transmitted equally often has the highest information content<sup>98</sup>. Here, an LMC's sensory information is maximised through pre- and postsynaptic morphodynamic processes, in which quantal refractory sampling jointly adapts to light stimulus changes, dynamically adjusting the synaptic gain (Figure 7A; cf. joint probability at each second of stimulation).

Comparable to LMCs, dynamic adapting scaling for information maximisation has been shown in blowfly H1 neurons' action potential responses (spikes) to changing light stimulus velocities<sup>99</sup>. These neurons reside in the lobula plate optic lobe, deeper in the brain, at least three synapses away from LMCs. Therefore, it is possible that H1s' adaptive dynamics partly project the earlier morphodynamic information sampling in the photoreceptor-LMC synapse or that adaptive rescaling is a general property of all neural systems<sup>100,101</sup>. Nevertheless, the continuously adapting weighted-average of the six variable photoreceptor responses reported independently to LMCs, combat noise and may carry the best (most accurate unbiased) running estimate of the ongoing light contrast signals. This *dynamic* maximisation of sensory information is distinct from Laughlin's original concept of *static* contrast equalisation<sup>102</sup>. The latter is based on stationary image statistics of a limited range and necessitates an implausible static synaptic encoder system<sup>35</sup> that imposes a constant synaptic gain. Furthermore, Laughlin's model does not address the issue of noise<sup>35</sup>.

Thus, ultrafast morphodynamics actively shapes neurons' macroscopic voltage response waveforms maximising information flow. These adaptive dynamics impact both the presynaptic quantal transmitter release and postsynaptic integration of the sampled quanta, influencing the underlying quantum bump size, latency, and refractory distributions<sup>12</sup>. Advantageously, intracellular microelectrode recordings in vivo provide a means to estimate these distributions statistically with high accuracy<sup>19,22,55,73</sup>. Knowing these distributions and the number of sampling units obtained from ultrastructural electron microscopy data, one can accurately predict neural responses and their information content for any stimulus patterns<sup>22,55,56,73,94</sup>. These 4-parameter quantal sampling models, which avoid the need for free parameters<sup>12,14,53,57,58</sup>, have been experimentally validated<sup>12,14,19,53,55,57,58,73,94</sup> (Figure 7C), providing a biophysically realistic multiscale framework to understand the involved neural computations<sup>12,58</sup>.

From a computational standpoint, a neural sampling or transmission system exerts adaptive quantum efficiency regulation that can be likened to division (cf. Text Box 1). Proportional quantal sample counting is achieved through motion-enhanced refractory transmission, sampling units, or combinations. This refractory adaptive mechanism permits a broad dynamic range, facilitating response normalisation through adaptive scaling and integration of quantal information<sup>12,14,56</sup>. Consequently, noise is minimised, leading to enhanced reliability of macroscopic responses<sup>12,56</sup>.

Therefore, we expect that this efficient information maximisation strategy, which has demonstrated signal-to-noise ratios reaching several thousand in insect photoreceptors during bright saccadic stimulation<sup>12,56</sup> (Figure 7C), will serve as a fundamental principle for neural computations involving the sampling of quantal bursts of information, such as neurotransmitter or odorant molecules. In this context, it is highly plausible that the pre- and postsynaptic morphodynamic quantal processes of neurons have co-adapted to convert logarithmic sample rate changes into precise phasic responses with limited amplitude and frequency distributions<sup>12,19</sup>, similar to the performance seen in fly photoreceptor<sup>12,14,53,55,73</sup> and first visual interneurons, LMCs<sup>19,22</sup>. Hence, ultrafast refractory quantal morphodynamics may represent a prerequisite for efficiently allocating information within the biophysically constrained amplitude and frequency ranges of neurons<sup>94,96,103</sup>.

### Predictive Coding and Minimal Neural Delays

Hopfield and Brody initially proposed that brain networks might employ transient synchrony as a collective mechanism for spatiotemporal integration for action potential communication<sup>104</sup>. Interestingly, morphodynamic quantal refractory information sampling and processing may offer the means to achieve this general coding objective.

Neural circuits incorporate predictive coding mechanisms that leverage mechanical, electrical, and synaptic feedback to minimise delays<sup>12,14,56</sup>. This processing, which enhances phasic inputs, synchronises the flow of information right from the first sampling stage<sup>12,19,35</sup>. It time-locks activity patterns into transient bursts of temporal scalability as observed in *Drosophila* photoreceptors' and LMCs' voltage responses to accelerating naturalistic light patterns (Figure 7D,E)<sup>12,35,104</sup>. Such phasic synchronisation and scalability are crucial for the brain to efficiently recognise and represent the changing world, irrespective of the animal's self-motion, and predict and lock onto its moving patterns. As a result, perception becomes more accurate, and behavioural responses to dynamic stimuli are prompt.

Crucially, this adaptive scalability of phasic, graded potential responses is readily translatable to sequences of action potentials (Figure 7E, cf. the scalable spike patterns predicted from the LMC responses). Thus, ultrafast neural morphodynamics may contribute to our brain's intrinsic ability to effortlessly capture the same meaning from a sentence, whether spoken very slowly or quickly. This dynamic form of predictive coding, which time-locks phasic neural responses to moving temporal patterns, differs markedly from the classic concept of interneurons using static centre-surround antagonism within their receptive fields to exploit spatial correlations in the natural scenes<sup>105</sup>.

Reinforcing fast morphodynamic synchronisation as a general phenomenon, we observe minimum phase responses deeper in the brain. In experiments involving tethered flying *Drosophila*, electrical activity patterns recorded from their lobula/lobula plate optic lobes<sup>86</sup> - at least three synapses downstream from photoreceptors - exhibit remarkably similar minimal delay responses to LMCs (Figure 8A), with the first responses emerging within 20 ms of the stimulus onset<sup>86</sup>. Such a rapid signal transmission through multiple neurons and synapses challenges traditional models that rely on the stationary eye and brain circuits with significant synaptic (chemical), signal integration and conduction (electrical) delays. Moreover, in vivo high-speed X-ray imaging<sup>14</sup> has revealed synchronised phasic movements across the *Drosophila* optic lobes following the rapid microsaccades of light-activated photoreceptors (Figure 8B). Synchronised tissue movements have also been observed during 2-photon imaging of optic lobe neurons<sup>14</sup> (Figure 8C). In the past, such movements have been often thought to be motion artefacts, with researchers making considerable efforts to eliminate them from calcium imaging data collection.

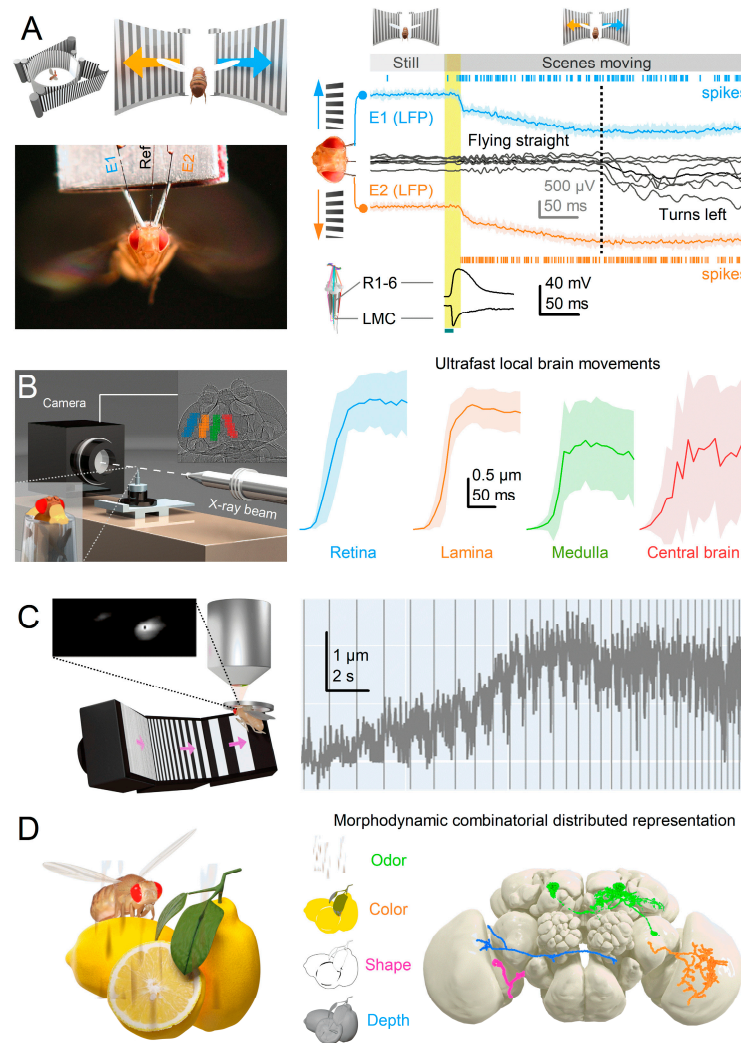


**Figure 8.** Synchronised minimal delay brain activity. (A) A *Drosophila* has 3 electrodes inserted into its brain: right (E1) and left (E2) lobula/lobula plate optic lobes and reference (Ref). It flies in a flight simulator seeing identical scenes of black and white stripes on its left and right<sup>86</sup>. When the scenes are still, the fly flies straight, and the right and left optic lobes show little activity; only a sporadic spike and the local field potentials (LFPs) are flat (E2, blue; E1, red traces). When the scenes start to sweep to the opposing directions, it takes less than 20 ms (yellow bar) for the optic lobes to respond to these visual stimuli (first spikes, and dips in LFPs). Interestingly, separate intracellular photoreceptor and large monopolar cell (LMC) recordings to 10 ms light pulse shows comparable time delays, peaking on average at 15 ms and 10 ms, respectively. Given that lobula and lobula plate neurons, which generate the observed spike and LFP patterns, are at least three synapses away from photoreceptors, the neural responses at different processing layers (retina, lamina, lobula plate) are closely synchronised, indicating minimal delays. Even though the fly brain has already received the visual information about the moving scenes, the fly makes little adjustments in its flight path, and the yaw torque remains flat. Only after minimum of 210 ms of stimulation, the fly finally chooses the left stimulus by attempting to turn left (dotted line), seen as intensifying yaw torque (downward). (B) Brief high-intensity X-ray pulses activate *Drosophila* photoreceptors<sup>14</sup>, causing photomechanical photoreceptor microsaccades across the eyes (characteristic retina movement). After a minute delay, also other parts of the brain move, shown for lamina, Medulla and Central brain. (C) During 2-photon imaging, L2-monopolar cell terminals can show mechanical jitter (grey noisy trace) that is synchronised with moving stimulus<sup>14</sup> (vertical stripes) (D) *Drosophila* brain networks may use multiple morphodynamic synchronised neural pathways to integrate a continuous (dynamically adjusted) combinatorial distributed neural representation of a lemon.

The absence of phasic amplification and synchronisation of signals through morphodynamics would have detrimental effects on communication speed and accuracy, resulting in slower perception and behavioural responses. It would significantly prolong the time it takes for visual information from the eyes to reach decision-making circuits, increasing uncertainty and leading to a decline in overall fitness. Thus, we expect the inherent scalability of neural morphodynamic responses (Figure 7D) to be crucial in facilitating efficient communication and synchronisation among different brain regions, enabling the coordination required for complex cognitive processes.

We propose that neurons exhibit morphodynamic jitter (stochastic oscillations) at the ultrastructural level sensitising the transmission system to achieve these concerted efforts. By enhancing phasic sampling, such jitter could minimise delays across the whole network, enabling interconnected circuits to respond in -sync to changes in information flow, actively co-differentiating the relevant (or attended) message stream<sup>86</sup>. Similarly, jitter-enhanced synchronisation could involve linking sensory (bottom-up) information about a moving object with the prediction (efference copy<sup>106,107</sup>) of movement-producing signals generated by the motor system, or top-down prediction of the respective self-motion<sup>108</sup>. Their difference signal, or prediction error, could then be used to rectify the animal's self-motion more swiftly than without the jitter-induced delay minimisation and synchronous phase enhancement, enabling faster behavioural responses.

We also expect ultrafast morphodynamics to contribute to multisensory integration by temporally aligning inputs from diverse sensory modalities with intrinsic goal-oriented processing (Figure 8D). This cross-modal synchronisation enhances behavioural certainty<sup>93,109</sup>. Using synchronised phasic information, a brain network can efficiently integrate yellow colour, shuttle-like shape, rough texture, and sweet scent into a unique neural representation, effectively identifying a *lemon* amidst the clutter and planning an appropriate action. These ultrafast combinatorial and distributed spatiotemporal responses expand the brain's capacity to encode information, increasing its representational dimensionality<sup>110</sup> beyond what could be achieved through slower processing in static circuits. Thus, the phasic nature of neural morphodynamics may enable animals to think and behave faster and more flexibly.

### Anti-aliasing and Robust Communication

Neural morphodynamics incorporates anti-aliasing sampling and signalling mechanisms within the peripheral nervous system<sup>12,14,111</sup> to prevent the distortion of sensory information. Like *Drosophila* compound eyes, photoreceptors in the primate retina exhibit varying sizes<sup>112</sup>, movements<sup>6</sup> and partially overlapping receptive fields<sup>113</sup>. Along with stochastic rhodopsin choices<sup>76</sup> (Figure 5B, inset), microstructural and synaptic variations<sup>114</sup>, these characteristics should create a stochastically heterogeneous sampling matrix free of spatiotemporal aliasing<sup>12,14,53,58</sup>. By enhancing sampling speed and phasic integration of changing information through heterogeneous channels, ultrafast morphodynamics reduces ambiguity in interpreting sensory stimuli and enhances the brain's "frame-rate" of perception. Such clear evolutionary benefits suggest that analogous morphodynamic processing would also be employed in central circuit processes for thinking and planning actions.

Furthermore, the inherent flexibility of neural morphodynamics using moving sampling units to collect and transmit information should help the brain maintain its functionality even when damaged, thus contributing to its resilience and recovery mechanisms. By using oscillating movements to enhance transmission and parallel information channels streaming overlapping content<sup>70</sup>, critical phasic information could potentially bypass or reroute around partially damaged neural tissue. This morphodynamic adaptability equips the brain to offset disturbances and continue information processing. As a result, brain morphodynamics ensures accurate sensory representation and bolsters neural communication's robustness amidst challenges or impairments.

### The Efficiency of Encoding Space in Time

Neural morphodynamics boosts the efficiency to encode space in time<sup>12,14</sup>, allowing smaller mobile sense organs - like compact compound eyes with fewer ommatidia - to achieve the spatial resolution equivalent to larger stationary sense organs (cf. Figures 5C and 6C). The resulting ultrafast

phasic sampling and transmission expedite sensory processing, while the reduced signal travel distance promotes faster perception, more efficient locomotion and decreases energy consumption. Therefore, we can postulate that between two brains of identical size, if one incorporates ultrafast morphodynamics across its neural networks while the other does not, the brain using morphodynamics has a higher information processing capacity. Its faster and more efficient information processing should enhance cognitive abilities and decision-making capabilities. In this light, for evolution to select neural morphodynamics as a pathway for optimising the brains would be a no-brainer.

### **Optimal Utilisation of Genetic Information in DNA**

Genetic information plays a crucial role in assembling the layout of the world representation during development and maturation within the brain tissue, with one outcome being the retainment of an animal's body coordinates with environmental patterns throughout the seemingly messy "neural spaghetti". By harnessing and fine-tuning genetic information, neural morphodynamics efficiently captures sensory information and utilises predetermined retinotopic or body-centric feature maps. This process facilitates perception and enables the emergence of sophisticated behavioural capabilities (Figures 5, 6 and 8), including hyperacute stereovision.

An animal's optimal functions and behaviours might be partially determined during the development of its brain network, with genetic information driving environmental simulations mediated by neural morphodynamics. This DNA-information-driven tuning of the morphodynamic brain's world map could explain why a newborn calf instinctively knows how to stand, locate its mother, and begin suckling. Conversely, during maturation and adulthood, brain morphodynamics allows the brain to dynamically adapt and reconfigure its local structures, optimising performance in response to changing environmental conditions and learning experiences.

However, it is the morphodynamic, electrical and chemical interplay of the neurons, which "animates" the brain's world representation, giving rise to thoughts and perceptions that continuously shape and transform the neural landscapes. Thus, as the ever-changing brain creates a projected reality of an ever-changing world, the underlying neural interplay makes it challenging to separate a neuron's form from its algorithmic function.

### **Future avenues of research**

Investigating the Integration of Ultrafast Morphodynamics Changes in the Brain and Behaviour  
One area of interest is understanding how the brain and behaviour can effectively synchronise with rapid morphodynamic changes, such as adaptive quantal sample rate modifications within the sensory receptor matrix and synaptic information transfer. A fundamental question pertains to how neural morphodynamics enhances the efficiency and speed of synaptic signal transmission. Is there a morphodynamic adaptation of synaptic vesicle sizes and quantities<sup>19</sup> that maximises information transfer? It is plausible that synaptic vesicle sizes and numbers adapt morphodynamically to ensure efficient information transfer, potentially using a running memory of the previous activity to optimise how transmitter molecule quantities scale in response to environmental information changes (cf. Figure 7A,B). This adaptive process might involve rapid exo- or endocytosis-linked movements of transmitter-receptor complexes. Furthermore, it is worthwhile to explore how brain morphodynamics adaptively regulates the synaptic cleft and optimises the proximity of neurotransmitter receptors to optimise signal transmission.

### **Genetically Enhancing Signalling Performance and Speed**

Another avenue of research involves investigating the possibility of genetically enhancing signalling performance and speed to control behaviours. This exploration can delve into how genetic

modifications may improve the efficiency and speed of signal processing in the brain. By manipulating genes to change neurons' physical properties, such as increasing the number of photoreceptor phototransduction units or neurotransmitter-receptor complexes or accelerating their biochemical reactions, it may be possible to enhance the performance and speed of signalling<sup>55,57</sup>, ultimately influencing behavioural responses. By further investigating these aspects of brain morphodynamics, we can gain deeper insights into the mechanisms underlying efficient information processing, synaptic signal transfer, and behavioural control.

For example, CRISPR-Cas9 gene-editing, by adding, removing, or altering specific genes associated with molecular motors or mechanoreceptive ion channels within neurons, provides means to elucidate these genes' functions and their roles in neural morphodynamics.

### Neural Activity Synchronisation

It is crucial to understand how neural morphodynamics synchronises brain activity within specific networks in a goal-directed manner and to comprehend the effects of changes in brain morphodynamics during maturation and learning on brain function and behaviour. Modern machine learning techniques now enable us to establish and quantify the contribution of brain morphodynamics to learning-induced structural and functional changes, and behaviour.

For instance, we can employ a deep learning approach to study how *Drosophila*'s compound eyes use photoreceptor movements to attain hyperacuity<sup>115</sup>. Could an artificial neural network (ANN), equipped with precisely positioned and photomechanically moving photoreceptors to process and transmit visual information to a lifelike-wired lamina connectome (cf. Figures 2 and 4), reproduce the natural response dynamics of real flies, thereby surpassing their optical pixelation limit? By systematically altering sampling dynamics and synaptic connections in an ANN-based compound eye model, it is now possible to test whether the performance falters without the realistic orientation-tuned photoreceptor movements and connectome and the eye loses its hyperacuity.

### Perception Enhancement

Neural morphodynamics mechanisms can enhance perception by implementing biomechanical feedback signals to photoreceptors via feedback synapses<sup>24</sup> to improve object detection against backgrounds. An object's movement makes detecting it from the background easier<sup>116</sup>. When interested in a particular object in a specific position, could the brain send attentive<sup>86,117</sup> feedback signals to a set of photoreceptors, in which receptive fields point at that position, to make them contract electromechanically, causing the object to 'jump'? This approach would enhance the object boundaries from its background<sup>118</sup>. Such biomechanical feedback would be the most efficient way to self-generate pop-up attention at the level of the sampling matrix.

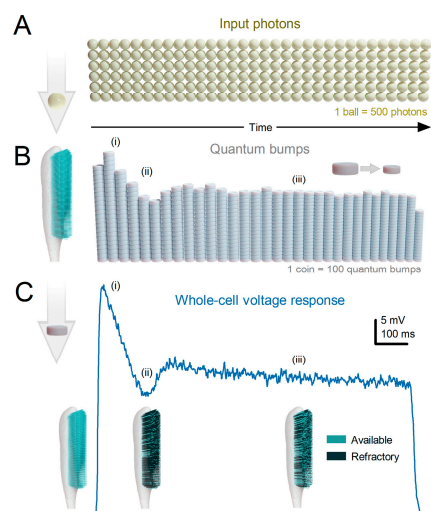
### Conclusion and future outlook

Theory of neural morphodynamics provides a new perspective that has a potential to revolutionise our understanding of brain function and behaviour. By addressing the key questions and conducting further research, we can explore the applications of ultrafast morphodynamics for neurotechnologies to enhance perception, improve artificial systems, and develop biomimetic devices and robots capable of sophisticated sensory processing and decision-making.

**Author Contributions:** MJ wrote the paper with content contributions from JT, JK, KRH, BS, JM and LC. All authors discussed and edited the manuscript.

**Acknowledgments:** We thank G. de Polavieja, G. Belušič, B. Webb, J. Howard, M. Göpfert, A. Lazar, P. Verkade, R. Mokso, S. Goodwin, M. Mangan, S.-C. Liu, P. Kuusela, R.C. Hardie and J Bennett for fruitful discussions. We thank G. de Polavieja, G. Belušič, S. Goodwin and R.C. Hardie for comments on the manuscript. This work was supported by BBSRC (BB/F012071/1 and BB/X006247/1) and EPSRC (EP/P006094/1 and EP/X019705/1) grants to MJ, Horizon Europe Framework Programme grant NimbleAI grant to LC, and BBSRC White-rose studentship (1945521) to BS.

**Declaration of Interests:** The authors declare no competing interests.



**Text Box 1: Visualising Refractory Quantal Computations.** By utilising powerful multi-scale morphodynamic neural models<sup>12,14,53</sup>, we can predict and analyse the generation and integration of voltage responses during morphodynamic quantal refractory sampling and compare these simulations to actual intracellular recordings for similar stimulation<sup>12,14,53</sup>. This approach, combined with information-theoretical analyses<sup>53,57,73,94</sup>, allows us to explain how phasic response waveforms arise from ultrafast movements and estimate the signal-to-noise ratio and information transfer rate of the neural responses. Importantly, these methods are applicable for studying the morphodynamic functions of any neural circuit. To illustrate the analytic power of this approach, we present a simple example: an intracellular recording (whole-cell voltage response) of dark-adapted *Drosophila* photoreceptors (TB1C) to a bright light pulse. See also Figure 2D that shows morphodynamic simulations of how a photoreceptor responds to two dots crossing its receptive field from east to west and west to east directions.

An insect photoreceptor's sampling units – e.g., 30,000 microvilli in a fruit fly or 90,000 in a blowfly R1-6 – count photons as variable samples (quantum bumps) and sum these up into a macroscopic voltage response, generating a reliable estimate of the encountered light stimulus. For clarity, visualise the light pulse as a consistent flow of photons, or golden balls, over time (TB1A). The quantum bumps that the photons elicit in individual microvilli can be thought of as silver coins of various sizes (TB1B). The photoreceptor is persistently counting these “coins” produced by its microvilli, thus generating a dynamically changing macroscopic response (TB1C, depicted as a blue trace). These basic counting rules<sup>119</sup> shape the photoreceptor response:

- Each microvillus can produce only one quantum bump at a time<sup>53,120-122</sup>.
- After producing a quantum bump, a microvillus becomes refractory for up to 300 ms (in *Drosophila* R1-6 photoreceptors at 25°C) and cannot respond to other photons<sup>120,123,124</sup>.
- Quantum bumps from all microvilli sum up the macroscopic response<sup>53,120-122,125</sup>.
- Microvilli availability sets a photoreceptor's maximum sample rate (quantum bump production rate), adapting its macroscopic response to a light stimulus<sup>53,122</sup>.
- Global Ca<sup>2+</sup> accumulation and membrane voltage affect samples of all microvilli. These global feedbacks strengthen with brightening light to reduce the size and duration of quantum bumps, adapting the macroscopic response<sup>55,73,126,127</sup>.

Adaptation in macroscopic response (TB1C) to continuous light (TB1A) is mostly caused by reduction in the number and size of quantum bumps over time (TB1B). When the stimulus starts, a large portion of the microvilli is simultaneously activated (TB1Ai and TB1Bi), but they subsequently enter a refractory state (TB1Aii and TB1Bii). This means that a smaller fraction of microvilli can respond to the following photons in the stimulus until more microvilli become available again. As a result, the number of activated microvilli initially reaches a peak and then rapidly declines, eventually settling into a steady state (TB1Aiii and TB1Biii) as the balance between photon arrivals and refractory periods is achieved. If all quantum bumps were identical, the macroscopic current



would simply reflect the number of activated microvilli based on the photon rate, resulting in a steady-state response. Light-induced current also exhibits a decaying trend towards lower plateau levels. This is because quantum bumps adapt to brighter backgrounds (TB1Aiii and TB1Biii), becoming smaller and briefer<sup>55,73</sup>. This adaptation is caused by global negative feedback, Ca<sup>2+</sup>-dependent inhibition of microvillar phototransduction reactions<sup>126-130</sup>. Additionally, the concurrent increase in membrane voltage compresses responses by reducing the electromotive force for the light-induced current across all microvilli<sup>53</sup>.

The signal-to-noise ratio and rate of information transfer increase with the average sampling rate, which is the average number of samples per unit time. Thus, the more samples that make up the macroscopic response to a given light pattern, the higher its information transfer rate. However, with more photons being counted by a photoreceptor at brightening stimulation, information about saccadic light patterns of natural scenes in its responses first increases and then approaches a constant rate. This is because:

(i) When more microvilli are in a refractory state, more photons fail to generate quantum bumps. As quantum efficiency drops, the equilibrium between used and available microvilli approaches a constant (maximum) quantum bump production rate (sample rate).

(ii) Once global Ca<sup>2+</sup> and voltage feedbacks saturate, they cannot make quantum bumps any smaller and briefer with increasing brightness.

(iii) After initial acceleration from the dark-adapted state, quantum bump latency distribution remains practically invariable in different light-adaptation states<sup>73</sup>.

Therefore, when sample rate modulation (i) and sample integration dynamics (ii and iii) of the macroscopic voltage responses settle (at intensities >10<sup>5</sup> photons/s in *Drosophila* R1-6 photoreceptors, allocation of visual information in the photoreceptor's amplitude and frequency range becomes nearly invariable<sup>53,57,131</sup>. Correspondingly, stochastic simulation closely predicts measured responses and rates of information transfer<sup>53,56,57</sup>. Notably, when the microvilli usage reaches a midpoint (~50 % level), the information rate encoded by the macroscopic responses to natural light intensity time series saturates<sup>53</sup>. This is presumably because sample rate modulation to light increments and decrements – which in the macroscopic response code for the number of different stimulus patterns<sup>94</sup> – saturate. Quantum bump size, if invariable, does not affect the information transfer rate – as long as the quantum bumps are briefer than the stimulus changes they encode. Thus, like any other filter, a fixed bump waveform affects signal and noise equally (data processing theorem<sup>53,94</sup>). But varying quantum bump size adds noise; when this variation is adaptive (memory-based), less noise is added<sup>53,94</sup>.

In summary, insect photoreceptors count photons through microvilli, integrate the responses, and adapt their macroscopic response based on the basic counting rules and global feedback mechanisms. The information transfer rate increases with the average sampling rate but eventually reaches a constant rate as the brightness of the stimulus increases. The size of the quantum bumps affects noise levels, with adaptive variation reducing noise.

## References

1. Eichler, K., Li, F., Litwin-Kumar, A., Park, Y., Andrade, I., Chneider-Mizell, C.M.S., Saumweber, T., Huser, A., Eschbach, C., Gerber, B., et al. (2017). The complete connectome of a learning and memory centre in an insect brain. *Nature* 548, 175-182. 10.1038/nature23455.
2. Oh, S.W., Harris, J.A., Ng, L., Winslow, B., Cain, N., Mihalas, S., Wang, Q.X., Lau, C., Kuan, L., Henry, A.M., et al. (2014). A mesoscale connectome of the mouse brain. *Nature* 508, 207-214. 10.1038/nature13186.
3. Rivera-Alba, M., Vitaladevuni, S.N., Mischenko, Y., Lu, Z.Y., Takemura, S.Y., Scheffer, L., Meinertzhagen, I.A., Chklovskii, D.B., and de Polavieja, G.G. (2011). Wiring economy and volume exclusion determine neuronal placement in the *Drosophila* brain. *Curr Biol* 21, 2000-2005. 10.1016/j.cub.2011.10.022.
4. Winding, M., Pedigo, B.D., Barnes, C.L., Patsolic, H.G., Park, Y., Kazimiers, T., Fushiki, A., Andrade, I.V., Khandelwal, A., Valdes-Aleman, J., et al. (2023). The connectome of an insect brain. *Science* 379, 995-1013. ARTN eadd9330 10.1126/science.add9330.
5. Hudspeth, A.J. (2008). Making an effort to listen: mechanical amplification in the ear. *Neuron* 59, 530-545. 10.1016/j.neuron.2008.07.012.

6. Pandiyan, V.P., Maloney-Bertelli, A., Kuchenbecker, J.A., Boyle, K.C., Ling, T., Chen, Z.C., Park, B.H., Roorda, A., Palanker, D., and Sabesan, R. (2020). The optoretinogram reveals the primary steps of phototransduction in the living human eye. *Sci Adv* 6. 10.1126/sciadv.abc1124.
7. Hardie, R.C., and Franze, K. (2012). Photomechanical responses in *Drosophila* photoreceptors. *Science* 338, 260-163. 10.1126/science.1222376.
8. Bocchero, U., Falleroni, F., Mortal, S., Li, Y., Cojoc, D., Lamb, T., and Torre, V. (2020). Mechanosensitivity is an essential component of phototransduction in vertebrate rods. *PLoS Biol* 18, e3000750. 10.1371/journal.pbio.3000750.
9. Korkotian, E., and Segal, M. (2001). Spike-associated fast contraction of dendritic spines in cultured hippocampal neurons. *Neuron* 30, 751-758. 10.1016/s0896-6273(01)00314-2.
10. Majewska, A., and Sur, M. (2003). Motility of dendritic spines in visual cortex in vivo: changes during the critical period and effects of visual deprivation. *Proc Natl Acad Sci U S A* 100, 16024-16029. 10.1073/pnas.2636949100.
11. Crick, F. (1982). Do dendritic spines twitch? *Trends in Neurosciences* 5, 44-46.
12. Juusola, M., Dau, A., Song, Z., Solanki, N., Rien, D., Jaciuch, D., Dongre, S.A., Blanchard, F., de Polavieja, G.G., Hardie, R.C., and Takalo, J. (2017). Microsaccadic sampling of moving image information provides *Drosophila* hyperacute vision. *Elife* 6. 10.7554/eLife.26117.
13. Kempainen, J., Mansour, N., Takalo, J., and Juusola, M. (2022). High-speed imaging of light-induced photoreceptor microsaccades in compound eyes. *Commun Biol* 5, 203. 10.1038/s42003-022-03142-0.
14. Kempainen, J., Scales, B., Razban Haghighi, K., Takalo, J., Mansour, N., McManus, J., Leko, G., Saari, P., Hurcomb, J., Antohi, A., et al. (2022). Binocular mirror-symmetric microsaccadic sampling enables *Drosophila* hyperacute 3D vision. *Proc Natl Acad Sci U S A* 119, e2109717119. 10.1073/pnas.2109717119.
15. Senthilan, P.R., Piepenbrock, D., Ovezmyradov, G., Nadrowski, B., Bechstedt, S., Pauls, S., Winkler, M., Mobius, W., Howard, J., and Gopfert, M.C. (2012). *Drosophila* auditory organ genes and genetic hearing defects. *Cell* 150, 1042-1054. 10.1016/j.cell.2012.06.043.
16. Reshetniak, S., and Rizzoli, S.O. (2021). The vesicle cluster as a major organizer of synaptic composition in the short-term and long-term. *Curr Opin Cell Biol* 71, 63-68. 10.1016/j.ceb.2021.02.007.
17. Reshetniak, S., Ussling, J.E., Perego, E., Rammner, B., Schikorski, T., Fornasiero, E.F., Truckenbrodt, S., Koster, S., and Rizzoli, S.O. (2020). A comparative analysis of the mobility of 45 proteins in the synaptic bouton. *Embo J* 39. ARTN e104596 10.15252/embj.2020104596.
18. Rusakov, D.A., Savtchenko, L.P., Zheng, K.Y., and Henley, J.M. (2011). Shaping the synaptic signal: molecular mobility inside and outside the cleft. *Trends Neurosci* 34, 359-369. 10.1016/j.tins.2011.03.002.
19. Juusola, M., Uusitalo, R.O., and Weckstrom, M. (1995). Transfer of graded potentials at the photoreceptor-interneuron synapse. *J Gen Physiol* 105, 117-148. 10.1085/jgp.105.1.117.
20. Fettiplace, R., Crawford, A.C., and Kennedy, H.J. (2006). Signal transformation by mechanotransducer channels of mammalian outer hair cells. *Auditory Mechanisms: Processes and Models*, 245-253. Doi 10.1142/9789812773456\_0043.
21. Kennedy, H.J., Crawford, A.C., and Fettiplace, R. (2005). Force generation by mammalian hair bundles supports a role in cochlear amplification. *Nature* 433, 880-883. 10.1038/nature03367.
22. Juusola, M., French, A.S., Uusitalo, R.O., and Weckstrom, M. (1996). Information processing by graded-potential transmission through tonically active synapses. *Trends Neurosci* 19, 292-297. 10.1016/S0166-2236(96)10028-X.
23. Watanabe, S., Rost, B.R., Camacho-Perez, M., Davis, M.W., Sohl-Kielczynski, B., Rosenmund, C., and Jorgensen, E.M. (2013). Ultrafast endocytosis at mouse hippocampal synapses. *Nature* 504, 242-247. 10.1038/nature12809.
24. Zheng, L., de Polavieja, G.G., Wolfram, V., Asyali, M.H., Hardie, R.C., and Juusola, M. (2006). Feedback network controls photoreceptor output at the layer of first visual synapses in *Drosophila*. *J Gen Physiol* 127, 495-510. 10.1085/jgp.200509470.
25. Shusterman, R., Smear, M.C., Koulakov, A.A., and Rinberg, D. (2011). Precise olfactory responses tile the sniff cycle. *Nat Neurosci* 14, 1039-1044. 10.1038/nn.2877.
26. Smear, M., Shusterman, R., O'Connor, R., Bozza, T., and Rinberg, D. (2011). Perception of sniff phase in mouse olfaction. *Nature* 479, 397-400. 10.1038/nature10521.
27. Bush, N.E., Solla, S.A., and Hartmann, M.J.Z. (2016). Whisking mechanics and active sensing. *Curr Opin Neurobiol* 40, 178-186. 10.1016/j.conb.2016.08.001.
28. Daghfous, G., Smargiassi, M., Libourel, P.A., Wattiez, R., and Bels, V. (2012). The function of oscillatory tongue-flicks in snakes: insights from kinematics of tongue-flicking in the banded water snake (*Nerodia fasciata*). *Chem Senses* 37, 883-896. 10.1093/chemse/bjs072.
29. van Hateren, J.H., and Schilstra, C. (1999). Blowfly flight and optic flow II. Head movements during flight. *J Exp Biol* 202, 1491-1500.
30. Schutz, A.C., Braun, D.I., and Gegenfurtner, K.R. (2011). Eye movements and perception: a selective review. *J Vis* 11. 10.1167/11.5.9.

31. Land, M. (2019). Eye movements in man and other animals. *Vis Res* 162, 1-7. 10.1016/j.visres.2019.06.004.
32. Davies, A., Louis, M., and Webb, B. (2015). A model of *Drosophila* larva chemotaxis. *Plos Comp Biol* 11. ARTN e1004606 10.1371/journal.pcbi.1004606.
33. Gomez-Marin, A., Stephens, G.J., and Louis, M. (2011). Active sampling and decision making in *Drosophila* chemotaxis. *Nature Comm* 2. ARTN 441 10.1038/ncomms1455.
34. Schoneich, S., and Hedwig, B. (2010). Hyperacute directional hearing and phonotactic steering in the cricket (*Gryllus bimaculatus* deGeer). *Plos One* 5. ARTN e15141 10.1371/journal.pone.0015141.
35. Zheng, L., Nikolaev, A., Wardill, T.J., O'Kane, C.J., de Polavieja, G.G., and Juusola, M. (2009). Network adaptation improves temporal representation of naturalistic stimuli in *Drosophila* eye: I dynamics. *PLoS One* 4, e4307. 10.1371/journal.pone.0004307.
36. Barlow, H.B. (1961). Possible principles underlying the transformations of sensory messages. In *Sensory Communication*, W. Rosenblith, ed. (M.I.T. Press), pp. 217-234.
37. Darwin, C. (1859). *On the origin of species by means of natural selection, or the preservation of favoured races in the struggle for life* (John Murray).
38. Sheehan, M.J., and Tibbetts, E.A. (2011). Specialized face learning is associated with individual recognition in paper wasps. *Science* 334, 1272-1275. 10.1126/science.1211334.
39. Miller, S.E., Legan, A.W., Henshaw, M.T., Ostevik, K.L., Samuk, K., Uy, F.M.K., and Sheehan, M.J. (2020). Evolutionary dynamics of recent selection on cognitive abilities. *Proc Natl Acad Sci U S A* 117, 3045-3052. 10.1073/pnas.1918592117.
40. Kacsoh, B.Z., Lynch, Z.R., Mortimer, N.T., and Schlenke, T.A. (2013). Fruit flies medicate offspring after seeing parasites. *Science* 339, 947-950. 10.1126/science.1229625.
41. Land, M.F. (1997). Visual acuity in insects. *Ann Rev Entomol* 42, 147-177. DOI 10.1146/annurev.ento.42.1.147.
42. Laughlin, S.B. (1989). The role of sensory adaptation in the retina. *J Exp Biol* 146, 39-62.
43. Laughlin, S.B., van Steveninck, R.R.D., and Anderson, J.C. (1998). The metabolic cost of neural information. *Nat Neurosci* 1, 36-41. Doi 10.1038/236.
44. Schilstra, C., and Van Hateren, J.H. (1999). Blowfly flight and optic flow I. Thorax kinematics and flight dynamics. *J Exp Biol* 202, 1481-1490.
45. Fenk, L.M., Avritzer, S.C., Weisman, J.L., Nair, A., Randt, L.D., Mohren, T.L., Siwanowicz, I., and Maimon, G. (2022). Muscles that move the retina augment compound eye vision in *Drosophila*. *Nature* 612, 116-122. 10.1038/s41586-022-05317-5.
46. Guiraud, M., Roper, M., and Chittka, L. (2018). High-speed videography reveals how honeybees can turn a spatial concept learning task into a simple discrimination task by stereotyped flight movements and sequential inspection of pattern elements. *Front Psychol* 9. 10.3389/fpsyg.2018.01347.
47. Nityananda, V., Skorupski, P., and Chittka, L. (2014). Can bees see at a glance? *J Exp Biol* 217, 1933-1939. 10.1242/jeb.101394.
48. Vasas, V., and Chittka, L. (2019). Insect-inspired sequential inspection strategy enables an artificial network of four neurons to estimate numerosity. *Iscience* 11, 85-92. 10.1016/j.isci.2018.12.009.
49. Chittka, L., and Skorupski, P. (2017). Active vision: A broader comparative perspective is needed. *Constr Found* 13, 128-129.
50. Sorribes, A., Armendariz, B.G., Lopez-Pigozzi, D., Murga, C., and de Polavieja, G.G. (2011). The origin of behavioral bursts in decision-making circuitry. *Plos Comput Biol* 7, e1002075. 10.1371/journal.pcbi.1002075.
51. Exner, S. (1891). *Die Physiologie der facettierten Augen von Krebsen und Insecten*.
52. Hardie, R.C., and Juusola, M. (2015). Phototransduction in *Drosophila*. *Curr Opin Neurobiol* 34, 37-45. 10.1016/j.conb.2015.01.008.
53. Song, Z., Postma, M., Billings, S.A., Coca, D., Hardie, R.C., and Juusola, M. (2012). Stochastic, adaptive sampling of information by microvilli in fly photoreceptors. *Curr Biol* 22, 1371-1380. 10.1016/j.cub.2012.05.047.
54. Stavenga, D.G. (2003). Angular and spectral sensitivity of fly photoreceptors. II. Dependence on facet lens F-number and rhabdomere type in *Drosophila*. *J Comp Physiol A* 189, 189-202. 10.1007/s00359-003-0390-6.
55. Juusola, M., and Hardie, R.C. (2001). Light Adaptation in *Drosophila* Photoreceptors: I. Response Dynamics and Signaling Efficiency at 25°C. *J Gen Physiol* 117, 3-25. DOI 10.1085/jgp.117.1.27.
56. Juusola, M., and Song, Z.Y. (2017). How a fly photoreceptor samples light information in time. *J Physiol Lond* 595, 5427-5437. 10.1113/jp273645.
57. Song, Z., and Juusola, M. (2014). Refractory sampling links efficiency and costs of sensory encoding to stimulus statistics. *J Neurosci* 34, 7216-7237. 10.1523/JNEUROSCI.4463-13.2014.
58. Song, Z., Zhou, Y., Feng, J., and Juusola, M. (2021). Multiscale 'whole-cell' models to study neural information processing - New insights from fly photoreceptor studies. *J Neurosci Methods* 357, 109156. 10.1016/j.jneumeth.2021.109156.

59. Gonzalez-Bellido, P.T., Wardill, T.J., and Juusola, M. (2011). Compound eyes and retinal information processing in miniature dipteran species match their specific ecological demands. *Proc Natl Acad Sci U S A* 108, 4224-4229. 10.1073/pnas.1014438108.
60. Juusola, M. (1993). Linear and nonlinear contrast coding in light-adapted blowfly photoreceptors. *J Comp Physiol A* 172, 511-521. Doi 10.1007/Bf00213533.
61. Ditchburn, R.W., and Ginsborg, B.L. (1952). Vision with a stabilized retinal image. *Nature* 170, 36-37. DOI 10.1038/170036a0.
62. Riggs, L.A., and Ratliff, F. (1952). The effects of counteracting the normal movements of the eye. *J Opt Soc Am* 42, 872-873.
63. Geurten, B.R.H., Jahde, P., Corthals, K., and Gopfert, M.C. (2014). Saccadic body turns in walking *Drosophila*. *Front Behav Neurosci* 8. ARTN 365 10.3389/fnbeh.2014.00365.
64. Borst, A. (2009). *Drosophila's* view on insect vision. *Curr Biol* 19, 36-47. 10.1016/j.cub.2008.11.001.
65. Franceschini, N., and Kirschfeld, K. (1971). Phenomena of pseudopupil in compound eye of *Drosophila*. *Kybernetik* 9, 159-182. Doi 10.1007/Bf02215177.
66. Woodgate, J.L., Makinson, J.C., Rossi, N., Lim, K.S., Reynolds, A.M., Rawlings, C.J., and Chittka, L. (2021). Harmonic radar tracking reveals that honeybee drones navigate between multiple aerial leks. *Iscience* 24. ARTN 102499 10.1016/j.isci.2021.102499.
67. Schulte, P., Zeil, J., and Sturzl, W. (2019). An insect-inspired model for acquiring views for homing. *Biol Cybern* 113, 439-451. 10.1007/s00422-019-00800-1.
68. Boeddeker, N., Dittmar, L., Sturzl, W., and Egelhaaf, M. (2010). The fine structure of honeybee head and body yaw movements in a homing task. *Proc R Soc Lond B Biol Sci* 277, 1899-1906. 10.1098/rspb.2009.2326.
69. Kirschfeld, K. (1973). [Neural superposition eye]. *Fortschr Zool* 21, 229-257.
70. Wardill, T.J., List, O., Li, X., Dongre, S., McCulloch, M., Ting, C.Y., O'Kane, C.J., Tang, S., Lee, C.H., Hardie, R.C., and Juusola, M. (2012). Multiple spectral inputs improve motion discrimination in the *Drosophila* visual system. *Science* 336, 925-931. 10.1126/science.1215317.
71. Song, B.M., and Lee, C.H. (2018). Toward a mechanistic understanding of color vision in insects. *Front Neur Circ* 12. ARTN 16 10.3389/fncir.2018.00016.
72. Johnston, R.J., and Desplan, C. (2010). Stochastic mechanisms of cell fate specification that yield random or robust outcomes. *Ann Rev Cell Dev Biol* 26, 689-719. 10.1146/annurev-cellbio-100109-104113.
73. Juusola, M., and Hardie, R.C. (2001). Light adaptation in *Drosophila* photoreceptors: II. Rising temperature increases the bandwidth of reliable signaling *J Gen Physiol* 117, 27-42.
74. Vasiliaskas, D., Mazzoni, E.O., Sprecher, S.G., Brodetskiy, K., Johnston, R.J., Lidder, P., Vogt, N., Celik, A., and Desplan, C. (2011). Feedback from rhodopsin controls rhodopsin exclusion in *Drosophila* photoreceptors. *Nature* 479, 108-112. 10.1038/nature10451.
75. Dippé, M.A.Z., and Wold, E.H. (1985). Antialiasing through stochastic sampling. *ACM SIGGRAPH Computer Graphics* 19, 69-78. <https://doi.org/10.1145/325165.325182>
76. Field, G.D., Gauthier, J.L., Sher, A., Greschner, M., Machado, T.A., Jepson, L.H., Shlens, J., Gunning, D.E., Mathieson, K., Dabrowski, W., et al. (2010). Functional connectivity in the retina at the resolution of photoreceptors. *Nature* 467, 673-677. 10.1038/nature09424.
77. Götz, K.G. (1968). Flight control in *Drosophila* by visual perception of motion. *Kybernetik* 6, 199-208.
78. Hengstenberg, R. (1971). Eye muscle system of housefly *Musca Domestica* .1. Analysis of clock spikes and their source. *Kybernetik* 9, 56-77. Doi 10.1007/Bf00270852.
79. Colonnier, F., Manecy, A., Juston, R., Mallot, H., Leitel, R., Floreano, D., and Viollet, S. (2015). A small-scale hyperacute compound eye featuring active eye tremor: application to visual stabilization, target tracking, and short-range odometry. *Bioinspir Biomim* 10. Artn 026002 10.1088/1748-3190/10/2/026002.
80. Viollet, S., Godiot, S., Leitel, R., Buss, W., Breugnot, P., Menouni, M., Juston, R., Expert, F., Colonnier, F., L'Eplattenier, G., et al. (2014). Hardware architecture and cutting-edge assembly process of a tiny curved compound eye. *Sensors-Basel* 14, 21702-21721. 10.3390/s141121702.
81. Talley, J., Pusdekar, J., Feltenberger, A., Ketner, N., Evers, J., Liu, M., Gosh, A., Palmer, S.E., Wardill, T.J., and Gonzalez-Bellido, P.T. (2023). Predictive saccades and decision making in the beetle-predating saffron robber fly. *Curr Biol* 33, 1-13. <https://doi.org/10.1016/j.cub.2023.06.019>.
82. de Polavieja, G.G. (2006). Neuronal algorithms that detect the temporal order of events. *Neural Comp* 18, 2102-2121.
83. Hassenstein, B., and Reichardt, W. (1956). Systemtheoretische Analyse der Zeit-, Reihenfolgen- und Vorzeichenauswertung bei der Bewegungsperzeption des Rüsselkäfers *Chlorophanus*. *Z Naturforsch* 11b, 513-524.
84. Barlow, H.B., and Levick, W.R. (1965). The mechanism of directionally selective units in rabbit's retina. *J Physiol* 178, 477-504. 10.1113/jphysiol.1965.sp007638.
85. Grabowska, M.J., Jeans, R., Steeves, J., and van Swinderen, B. (2020). Oscillations in the central brain of *Drosophila* are phase locked to attended visual features. *Proc Natl Acad Sci U S A* 117, 29925-29936. 10.1073/pnas.2010749117.

86. Tang, S., and Juusola, M. (2010). Intrinsic activity in the fly brain gates visual information during behavioral choices. *PLoS One* 5, e14455. 10.1371/journal.pone.0014455.
87. Leung, A., Cohen, D., van Swinderen, B., and Tsuchiya, N. (2021). Integrated information structure collapses with anesthetic loss of conscious arousal in *Drosophila melanogaster*. *Plos Comput Biol* 17, e1008722. 10.1371/journal.pcbi.1008722.
88. Chiappe, M.E., Seelig, J.D., Reiser, M.B., and Jayaraman, V. (2010). Walking modulates speed sensitivity in *Drosophila* motion vision. *Curr Biol* 20, 1470-1475. 10.1016/j.cub.2010.06.072.
89. Maimon, G., Straw, A.D., and Dickinson, M.H. (2010). Active flight increases the gain of visual motion processing in *Drosophila*. *Nat Neurosci* 13, 393-399. 10.1038/nn.2492.
90. Maye, A., Hsieh, C.H., Sugihara, G., and Brembs, B. (2007). Order in spontaneous behavior. *PLoS One* 2, e443. 10.1371/journal.pone.0000443.
91. van Hateren, J.H. (2017). A unifying theory of biological function. *Biol Theory* 12, 112-126. 10.1007/s13752-017-0261-y.
92. van Hateren, J.H. (2019). A theory of consciousness: computation, algorithm, and neurobiological realization. *Biol Cybern* 113, 357-372. 10.1007/s00422-019-00803-y.
93. Okray, Z., Jacob, P.F., Stern, C., Desmond, K., Otto, N., Talbot, C.B., Vargas-Gutierrez, P., and Waddell, S. (2023). Multisensory learning binds neurons into a cross-modal memory engram. *Nature* 617, 777-784. <https://doi.org/10.1038/s41586-023-06013-8>.
94. Juusola, M., and de Polavieja, G.G. (2003). The rate of information transfer of naturalistic stimulation by graded potentials. *J Gen Physiol* 122, 191-206. 10.1085/jgp.200308824.
95. de Polavieja, G.G. (2002). Errors drive the evolution of biological signalling to costly codes. *J Theor Biol* 214, 657-664.
96. de Polavieja, G.G. (2004). Reliable biological communication with realistic constraints. *Phys Rev E* 70, 061910.
97. Li, X., Abou Tayoun, A., Song, Z., Dau, A., Rien, D., Jaciuch, D., Dongre, S., Blanchard, F., Nikolaev, A., Zheng, L., et al. (2019). Ca<sup>2+</sup>-activated K<sup>+</sup> channels reduce network excitability, improving adaptability and energetics for transmitting and perceiving sensory information. *J Neurosci* 39, 7132-7154. 10.1523/JNEUROSCI.3213-18.2019.
98. Shannon, C.E. (1948). A mathematical theory of communication. *Bell Syst Technic J* 27, 379-423, 623-656.
99. Brenner, N., Bialek, W., and de Ruyter van Steveninck, R. (2000). Adaptive rescaling maximizes information transmission. *Neuron* 26, 695-702. 10.1016/s0896-6273(00)81205-2.
100. Maravall, M., Petersen, R.S., Fairhall, A.L., Arabzadeh, E., and Diamond, M.E. (2007). Shifts in coding properties and maintenance of information transmission during adaptation in barrel cortex. *PLoS Biol* 5, e19. 10.1371/journal.pbio.0050019.
101. Arganda, S., Guantes, R., and de Polavieja, G.G. (2007). Sodium pumps adapt spike bursting to stimulus statistics. *Nat Neurosci* 10, 1467-1473. 10.1038/nn1982.
102. Laughlin, S.B. (1981). A simple coding procedure enhances a neuron's information capacity. *Zeitschrift für Naturforschung C* 36, 910-912.
103. van Hateren, J.H. (1992). A theory of maximizing sensory information. *Biol Cybern* 68, 23-29. 10.1007/BF00203134.
104. Hopfield, J.J., and Brody, C.D. (2001). What is a moment? Transient synchrony as a collective mechanism for spatiotemporal integration. *Proc Natl Acad Sci U S A* 98, 1282-1287. DOI 10.1073/pnas.031567098.
105. Srinivasan, M.V., Laughlin, S.B., and Dubs, A. (1982). Predictive coding: a fresh view of inhibition in the retina. *Proc R Soc Lond B Biol Sci* 216, 427-459. 10.1098/rspb.1982.0085.
106. Poulet, J.F., and Hedwig, B. (2006). The cellular basis of a corollary discharge. *Science* 311, 518-522. 10.1126/science.1120847.
107. Poulet, J.F., and Hedwig, B. (2007). New insights into corollary discharges mediated by identified neural pathways. *Trends Neurosci* 30, 14-21. 10.1016/j.tins.2006.11.005.
108. Fujiwara, T., Cruz, T.L., Bohoslav, J.P., and Chiappe, M.E. (2017). A faithful internal representation of walking movements in the *Drosophila* visual system. *Nat Neurosci* 20, 72-81. 10.1038/nn.4435.
109. Solvi, C., Al-Khudhairy, S.G., and Chittka, L. (2020). Bumble bees display cross-modal object recognition between visual and tactile senses. *Science* 367, 910-912. 10.1126/science.aay8064.
110. Badre, D., Bhandari, A., Keglovits, H., and Kikumoto, A. (2021). The dimensionality of neural representations for control. *Curr Opin Behav Sci* 38, 20-28. 10.1016/j.cobeha.2020.07.002.
111. Yellott, J.I. (1982). Spectral-analysis of spatial sampling by photoreceptors - topological disorder prevents aliasing. *Vis Res* 22, 1205-1210. Doi 10.1016/0042-6989(82)90086-4.
112. Wikler, K.C., and Rakic, P. (1990). Distribution of photoreceptor subtypes in the retina of diurnal and nocturnal primates. *J Neurosci* 10, 3390-3401. 10.1523/JNEUROSCI.10-10-03390.1990.
113. Kim, Y.J., Peterson, B.B., Crook, J.D., Joo, H.R., Wu, J., Puller, C., Robinson, F.R., Gamlin, P.D., Yau, K.W., Viana, F., et al. (2022). Origins of direction selectivity in the primate retina. *Nat Commun* 13, 2862. 10.1038/s41467-022-30405-5.

114. Yu, W.Q., Swanstrom, R., Sigulinsky, C.L., Ahlquist, R.M., Knecht, S., Jones, B.W., Berson, D.M., and Wong, R.O. (2023). Distinctive synaptic structural motifs link excitatory retinal interneurons to diverse postsynaptic partner types. *Cell Rep* 42, 112006. 10.1016/j.celrep.2023.112006.
115. Razban Haghighi, K. (2023). The *Drosophila* visual system: a super-efficient encoder. PhD (University of Sheffield).
116. Kapustjansky, A., Chittka, L., and Spaethe, J. (2010). Bees use three-dimensional information to improve target detection. *Naturwissenschaften* 97, 229-233. 10.1007/s00114-009-0627-5.
117. van Swinderen, B. (2011). Attention in *Drosophila*. *Int Rev Neurobiol* 99, 51-85. 10.1016/B978-0-12-387003-2.00003-3.
118. Chittka, L., and Spaethe, J. (2007). Visual search and the importance of time in complex decision making by bees. *Arthropod-Plant Inte* 1, 37-44. 10.1007/s11829-007-9001-8.
119. Juusola, M., Song, Z., and Hardie, R.C. (2022). Phototransduction Biophysics. In *Encyclopedia of Computational Neuroscience*, D. Jaeger, and R. Jung, eds. (Springer), pp. 2758-2776. [https://doi.org/10.1007/978-1-0716-1006-0\\_333](https://doi.org/10.1007/978-1-0716-1006-0_333).
120. Hochstrate, P., and Hamdorf, K. (1990). Microvillar components of light adaptation in blowflies. *J Gen Physiol* 95, 891-910. 10.1085/jgp.95.5.891.
121. Pumir, A., Graves, J., Ranganathan, R., and Shraiman, B.I. (2008). Systems analysis of the single photon response in invertebrate photoreceptors. *Proc Natl Acad Sci U S A* 105, 10354-10359. 10.1073/pnas.0711884105.
122. Howard, J., Blakeslee, B., and Laughlin, S.B. (1987). The intracellular pupil mechanism and photoreceptor signal: noise ratios in the fly *Lucilia cuprina*. *Proc R Soc Lond B Biol Sci* 231, 415-435. 10.1098/rspb.1987.0053.
123. Mishra, P., Socolich, M., Wall, M.A., Graves, J., Wang, Z., and Ranganathan, R. (2007). Dynamic scaffolding in a G protein-coupled signaling system. *Cell* 131, 80-92. 10.1016/j.cell.2007.07.037.
124. Scott, K., Sun, Y., Beckingham, K., and Zuker, C.S. (1997). Calmodulin regulation of *Drosophila* light-activated channels and receptor function mediates termination of the light response in vivo. *Cell* 91, 375-383. 10.1016/s0092-8674(00)80421-3.
125. Liu, C.H., Satoh, A.K., Postma, M., Huang, J., Ready, D.F., and Hardie, R.C. (2008). Ca<sup>2+</sup>-dependent metarhodopsin inactivation mediated by calmodulin and NINAC myosin III. *Neuron* 59, 778-789. 10.1016/j.neuron.2008.07.007.
126. Wong, F., and Knight, B.W. (1980). Adapting-bump model for eccentric cells of *Limulus*. *J Gen Physiol* 76, 539-557. 10.1085/jgp.76.5.539.
127. Wong, F., Knight, B.W., and Dodge, F.A. (1980). Dispersion of latencies in photoreceptors of *Limulus* and the adapting-bump model. *J Gen Physiol* 76, 517-537. 10.1085/jgp.76.5.517.
128. Hardie, R.C., and Postma, M. (2008). Phototransduction in microvillar photoreceptors of *Drosophila* and other invertebrates. In *The senses: a comprehensive reference*. Vision, A.I. Basbaum, A. Kaneko, G.M. Shepherd, and G. Westheimer, eds. (Academic), pp. 77-130.
129. Postma, M., Oberwinkler, J., and Stavenga, D.G. (1999). Does Ca<sup>2+</sup> reach millimolar concentrations after single photon absorption in *Drosophila* photoreceptor microvilli? *Biophys J* 77, 1811-1823. 10.1016/S0006-3495(99)77026-8.
130. Hardie, R.C. (1996). INDO-1 measurements of absolute resting and light-induced Ca<sup>2+</sup> concentration in *Drosophila* photoreceptors. *J Neurosci* 16, 2924-2933. 10.1523/JNEUROSCI.16-09-02924.1996.
131. Faivre, O., and Juusola, M. (2008). Visual coding in locust photoreceptors. *Plos One* 3. ARTN e2173 10.1371/journal.pone.0002173.

**Disclaimer/Publisher's Note:** The statements, opinions and data contained in all publications are solely those of the individual author(s) and contributor(s) and not of MDPI and/or the editor(s). MDPI and/or the editor(s) disclaim responsibility for any injury to people or property resulting from any ideas, methods, instructions or products referred to in the content.